Liquids and Gases in Motion; Fluid Dynamics

8

W. Demtröder, *Mechanics and Thermodynamics*, Undergraduate Lecture Notes in Physics, DOI 10.1007/978-3-319-27877-3_8

Chapter 8

Up to now we have only considered liquids and gases at rest where the total momentum $\boldsymbol{P} = \sum \boldsymbol{p}_i = \boldsymbol{0}$, although the momenta p_i of the individual molecules, because of their thermal motion, are not zero but show a Maxwellian distribution with directions uniformly spread over all directions.

In this chapter, we will discuss phenomena that occur for streaming liquids and gases. Their detailed investigation has led to a special research area, the **hydrodynamics** resp. **aerodynamics** which are treated in more detail in special textbooks [8.1a–8.3b].

The macroscopic treatment of fluids in motion generally neglects the thermal motion of the individual molecules but considers only the average motion of a volume element ΔV, which can depend on the position $\boldsymbol{r} = \{x, y, z\}$. Since even for very small volume elements with dimensions in the mm-range ΔV still contains about 10^{15} molecules, the averaging is justified. The main difference between streaming fluids and gases is the density, which differs by about 3 orders of magnitude. This is closely related to the incompressibility of liquids while gases can be readily compressed. For streaming liquids, the density ϱ is constant in time, while the gas density can vary with time and position.

A complete description of the macroscopic motion of liquids and gases demands the knowledge of all forces acting on a volume element ΔV with the mass $\Delta m = \varrho \cdot \Delta V$. These forces have different underlying causes:

- pressure differences between different local positions induce forces $\boldsymbol{F}_\mathrm{p} = -\mathbf{grad}\, p \cdot \Delta V$ on a volume element ΔV.
- The gravity force $F_g = \Delta m \cdot g = \varrho \cdot g \cdot \Delta V$ leads for fluid flows with a vertical component to acceleration of ΔV.
- If the flow velocity u depends on the position $\boldsymbol{r}$ this results in friction forces F_f between layers of the fluid flow with different values of u.
- Charged particles in streaming fluids experience additional forces by external electric or magnetic fields (Lorentz force see Vol. 2). Such forces play an important role in stars and in laboratory plasmas. They are therefore extensively investigated in Plasmaphysics and Astrophysics. We will discuss them here, however, no longer, because their treatment is the subject of magneto-hydrodynamics and it would exceed the frame of the present textbook.

The Newtonian equation for the motion of a mass element $\Delta m = \varrho \cdot \Delta V$ in motion is then

$$\begin{aligned} \boldsymbol{F} &= \boldsymbol{F}_p + \boldsymbol{F}_g + \boldsymbol{F}_\mathrm{f} = \Delta m \ddot{\boldsymbol{r}} \\ &= \varrho \cdot \Delta V \cdot \frac{\mathrm{d}\boldsymbol{u}}{\mathrm{d}t} \,, \end{aligned} \tag{8.1}$$

where $u = \mathrm{d}r/\mathrm{d}t$ is the flow velocity of the volume element ΔV.

Before we try to solve this equation we will discuss at first some basic definitions and features of fluids in motion.

8.1 Basic Definitions and Types of Fluid Flow

The motion of the whole liquid is known, if it is possible to define the flow velocity $\boldsymbol{u}(r, t)$ of an arbitrary volume element $\mathrm{d}V$ at every location r and at any time t (Fig. 8.1). All values $u(r, t_0)$ for a given time t_0 form the *velocity field* (also named *flow field*) which can change with time. If $u(r)$ does not depend on time, the velocity field is stationary.

For a stationary flow the velocity $u(r)$ is at any position $\boldsymbol{r}$ temporally constant. It can, however, differ for different locations $\boldsymbol{r}$ (Fig. 8.1b).

The location curve $\boldsymbol{r}(t)$, which is traversed by a volume element ΔV (e.g. visualized by a small piece of cork) is called its *streamline* or *stream filament* (Fig. 8.1). The density of streamlines is the number of streamlines passing per second through an area of 1 m^2. All streamlines passing through the area A form a **stream tube**. Since the liquid is always moving along the stream lines no liquid leaks out of the walls of a stream tube.

For a stationary flow the path $\boldsymbol{r}(t)$ of a volume element $\mathrm{d}V$ follows the curve $\boldsymbol{u}(\boldsymbol{r})$ of the flow field. For non-stationary flows ($\partial u/\partial t \neq 0$), this is generally not the case as is illustrated in Fig. 8.2, where the curve $u(r, t_1)$ of the velocity field at time t_1 extends from P_1 via P_2 to P_3. However, when the volume element $\mathrm{d}V$ has arrived in P_2 at the time $t_1 + \Delta t$, the velocity field has changed meanwhile and the volume element follows now the curve $u(r, t_1 + \Delta t)$ from P_2 to P_4.

Since the different forces in (8.1) generally have different directions and furthermore the friction force depends on the velocity gradient the motion of $\mathrm{d}V$ depends on the relative contribution

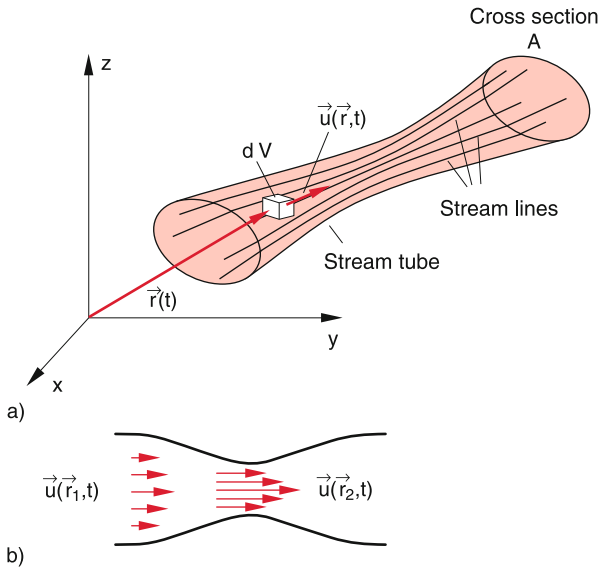

Figure 8.1 **a** Stream line, stream tube and flow velocity $u(\boldsymbol{r}, t)$; **b** Momentary condition of a flow field (velocity field)

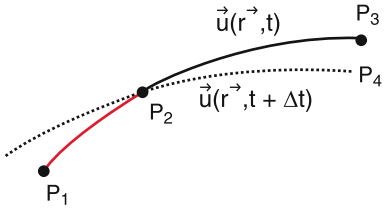

Figure 8.2 In a nonstationary flow the path of a particle does not necessarily follow a streamline $u(r, t)$

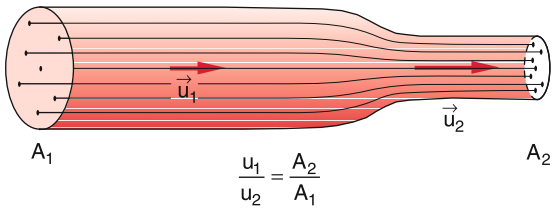

Figure 8.3 Example of a laminar flow

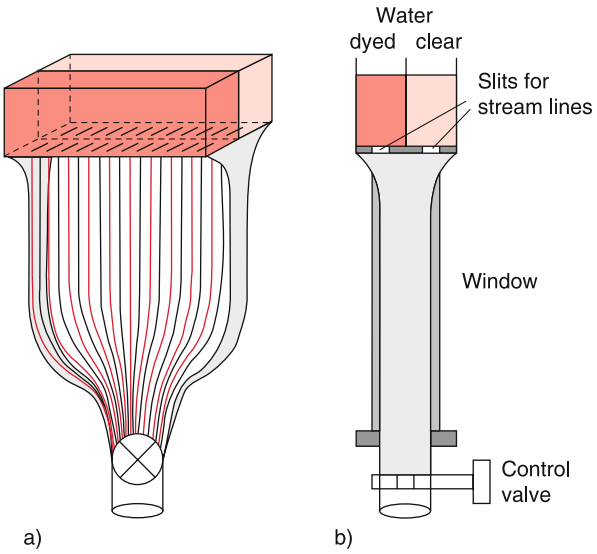

Figure 8.4 Streamline apparatus. **a** Angle view, **b** Side view

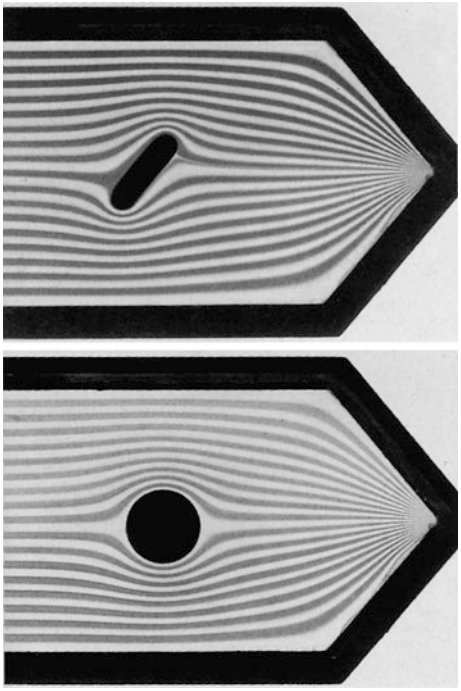

Figure 8.5 Laminar flow from left to right around different obstacles, photographed with the streamline device of Fig. 8.4

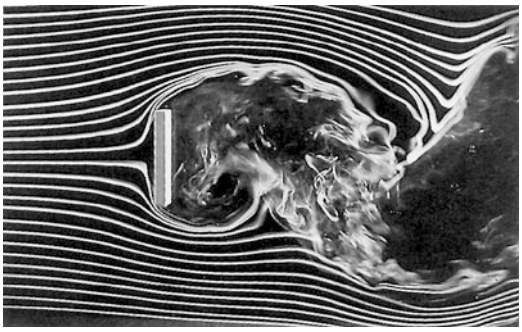

Figure 8.6 A laminar flow coming from left becomes turbulent after impinging on a plate

of the different forces. Liquids where the friction forces are negligible compared to the other forces are called **ideal liquids**. If the frictional forces are large compared to all other forces we have the limiting case of viscous liquids.

Examples for the first case are the flow of liquid helium through a pipe or of air along the smooth wing of an airplane, while the second case is realized by the flow of honey or molasses out of a sloped glass container onto a slice of bread or the slow flow of heavy oil through pipelines. The real liquids and gases are located between these two limiting cases. A flow where the stream lines stay side by side without mixing is called a **laminar flow** (Fig. 8.3). Laminar flows are always realized if the frictional forces are dominant. They can be demonstrated with the streamline generator. This is an apparatus where the bottom of two containers has narrow slits arranged in such a way, that the liquid from each container streams alternately through every second slit downwards between two parallel glass plates (Fig. 8.4). When one container is filled with red dyed water and the other with black tinted water the stream lines are alternately black and red. With such a demonstration apparatus the stream line conditions with different obstacles in the flow can be readily shown to a large auditorium, if projected onto a large screen (Fig. 8.5).

Turbulent flows are generated by friction between the wall and the peripheral layer of the flow if the internal friction of the flow is smaller than the accelerating forces. Vortices are formed which can intermixe the stream lines completely (Fig. 8.6).

8.2 Euler Equation for Ideal Liquids

A volume element dV with the flow velocity $\boldsymbol{u}(\boldsymbol{r}, t)$ passes during the time interval dt a path length $d\boldsymbol{r} = \boldsymbol{u}dt$. Starting from the position r it reaches the position $\boldsymbol{r} + \boldsymbol{u} \cdot dt$ at time $t + dt$ and has there the velocity

$$\boldsymbol{u} + d\boldsymbol{u} = \boldsymbol{u}(\boldsymbol{r} + \boldsymbol{u}\, dt, t + dt) \,. \tag{8.2}$$

Even for stationary flows, the velocity can change with position. For example, a liquid flowing through a pipe increases its velocity when the pipe cross section decreases (Fig. 8.3). The stream line density is there increased. For nonstationary flows the velocity changes also with time even at the same location, because $\partial \boldsymbol{u}/dt \neq 0$.

We define the substantial acceleration of a volume element dV as the total change of its velocity $\boldsymbol{u} = \{u_x, u_y, u_z\}$ when dV passes during the time interval dt from the position $\boldsymbol{r}$ to $\boldsymbol{r} + d\boldsymbol{r}$. This total acceleration has two contributions:

1. the temporal change $\partial \boldsymbol{u}/\partial t$ at the same position
2. the change of u when dV passes from $\boldsymbol{r}$ to $\boldsymbol{r}+d\boldsymbol{r}$. This change is per second $(\partial \boldsymbol{u}/\partial \boldsymbol{r}) \cdot (\partial \boldsymbol{r}/\partial t)$.

This can be written in components as

$$\frac{du_x}{dt} = \frac{\partial u_x}{\partial t} + \frac{\partial u_x}{\partial x}\frac{dx}{dt} + \frac{\partial u_x}{\partial y}\frac{dy}{dt} + \frac{\partial u_x}{\partial z}\frac{dz}{dt} \tag{8.3a}$$

with corresponding equations for the other components u_y and u_z.

In vector form this reads with $u_x = dx/dt$, $u_y = dy/dt$, $u_z = dz/dt$

$$\frac{d\boldsymbol{u}}{dt} = \frac{\partial \boldsymbol{u}}{\partial t} + (\boldsymbol{u} \cdot \nabla)\,\boldsymbol{u} \,. \tag{8.3b}$$

Here $\boldsymbol{u} \cdot \nabla \boldsymbol{u}$ is the scalar product of the vector $\boldsymbol{u}$ and the tensor

$$\nabla \boldsymbol{u} = \begin{pmatrix} \frac{\partial u_x}{\partial x} & \frac{\partial u_x}{\partial y} & \frac{\partial u_x}{\partial z} \\ \frac{\partial u_y}{\partial x} & \frac{\partial u_y}{\partial y} & \frac{\partial u_y}{\partial z} \\ \frac{\partial u_z}{\partial x} & \frac{\partial u_z}{\partial y} & \frac{\partial u_z}{\partial z} \end{pmatrix} .$$

The substantial acceleration is composed of the time derivative $\partial \boldsymbol{u}/\partial t$ of the velocity at a fixed position r and the convection acceleration $(\boldsymbol{u} \cdot \nabla)\boldsymbol{u}$. The first contribution is only nonzero for nonstationary flows, the second only if the velocity changes with the position r.

The equation of motion for an ideal liquid (frictional forces are negligible) which experiences the accelerating forces of gravity $F_g = m \cdot \boldsymbol{g}$ and pressure gradient $\boldsymbol{F}_p = -\mathbf{grad}\, p \cdot dV$ is the **Euler equation**

$$\frac{d\boldsymbol{u}}{dt} = \frac{\partial \boldsymbol{u}}{\partial t} + (\boldsymbol{u} \cdot \nabla)\,\boldsymbol{u} = \boldsymbol{g} - \frac{1}{\varrho}\mathbf{grad}\, p \,. \tag{8.4}$$

This is the basic equation for the motion of ideal liquids, which was already postulated by L. Euler in 1755.

8.3 Continuity Equation

We consider a liquid volume $dV = A \cdot dx$, which flows in x-direction through a pipe with variable cross section $A(x)$ (Fig. 8.7a). Its mass is $dM = \varrho \cdot dV = \varrho \cdot A \cdot dx$. Through the cross section A_1 flows per time unit the mass

$$\frac{dM}{dt} = \varrho A_1 \frac{dx}{dt} = \varrho A_1 u_{x_1} \,. \tag{8.5}$$

We assume, that at the position $x = x_0$ the cross section A changes to A_2. For incompressible liquids ϱ remains constant. Since the liquid cannot escape through the side walls the mass flowing per time unit through A_2 must be equal to that flowing through A_1. This gives the equation

$$\varrho A_1 u_{x_1} = \varrho A_2 u_{x_2} \Rightarrow \frac{u_{x_1}}{u_{x_2}} = \frac{A_2}{A_1} \,. \tag{8.6}$$

Through the narrow part of the pipe the liquid flows faster than through a wide part. The product

$$\boldsymbol{j} = \varrho \cdot \boldsymbol{u} \tag{8.7}$$

is called **mass flow density**. The product $I = \boldsymbol{j} \cdot \boldsymbol{A}$ is the **total mass flow** and gives the mass flowing per unit time through the cross section $\boldsymbol{A}$.

Equation 8.6 can then be written as $I = \text{const}$. The total mass flow through a pipe is the same at every position in the pipe.

This statement about the conservation of the total mass flow can be formulated in a more general way: The volume V contains at

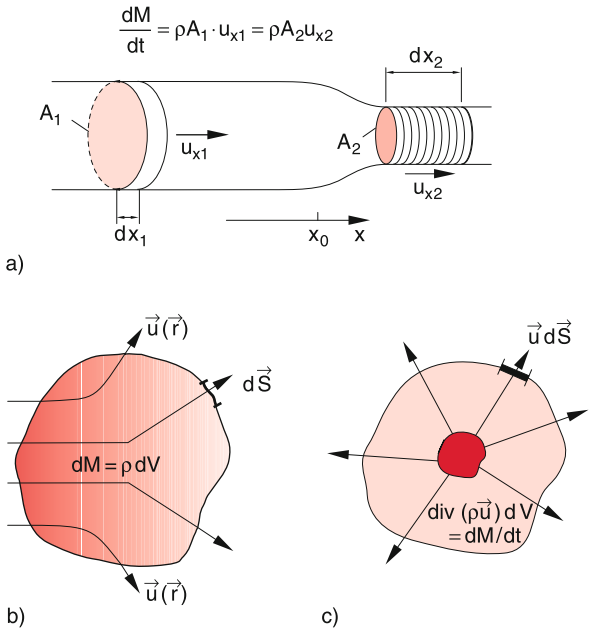

Figure 8.7 Illustration of the continuity equation: **a** in a pipe with changing diameter; **b** in a volume V with surface S with a mass flow dM/dt through V; **c** with a source inside a volume V

time t the liquid mass

$$M = \int_V \varrho \, \mathrm{d}V \, . \tag{8.8}$$

The mass per volume changes with time if mass flows out of the volume or into the volume. The mass flowing per second through its surface S is

$$-\frac{\partial M}{\partial t} = \int_S \varrho \cdot \boldsymbol{u} \, \mathrm{d}\boldsymbol{S} = \int_S \boldsymbol{j} \, \mathrm{d}\boldsymbol{S} \, , \tag{8.9}$$

where the normal vector $\mathrm{d}\boldsymbol{S}$ is perpendicular to the surface element $\mathrm{d}A$.

According to Gauß' law (see textbooks on vector analysis e.g. [8.8]) the surface integral can be converted into a volume integral over the volume V enclosed by the surface S.

$$\int_S \varrho \cdot \boldsymbol{u} \cdot \mathrm{d}\boldsymbol{S} = \int_V \mathrm{div}(\varrho \cdot \boldsymbol{u}) \mathrm{d}V \, , \tag{8.10}$$

and we obtain from (8.8)–(8.10) for a constant volume V the relation

$$-\frac{\partial}{\partial t} \int_V \varrho \, \mathrm{d}V = -\int \frac{\partial \varrho}{\partial t} \mathrm{d}V = \int \mathrm{div}(\varrho \boldsymbol{u}) \mathrm{d}V \, . \tag{8.11}$$

Since this must be valid for arbitrary volumes this gives the continuity equation

$$\frac{\partial \varrho}{\partial t} + \mathrm{div}(\varrho \boldsymbol{u}) = 0 \, , \tag{8.12}$$

which states that for any mass flow the total mass is conserved, i.e. **mass is neither produced nor annihilated**.

For a constant volume element $\mathrm{d}V$ (8.12) can be written as

$$\mathrm{div}(\varrho \cdot \boldsymbol{u}) \mathrm{d}V = -\frac{\partial \varrho}{\partial t} \mathrm{d}V = -\frac{\partial}{\partial t} (\mathrm{d}M) \, . \tag{8.12a}$$

The expression $\mathrm{div}(\varrho \cdot u) \cdot \mathrm{d}V$ gives the mass that escapes per second out of the volume element $\mathrm{d}V$. Therefore $\mathrm{div}(\varrho \cdot \boldsymbol{u})$ is called the **source strength** per unit volume. A source which delivers the mass $\mathrm{d}M/\mathrm{d}t$ per sec leads to a mass flow $\mathrm{div}(\varrho \cdot u)$ per sec through the surface surrounding the source (Fig. 8.7c).

The continuity equation (8.12) is valid for liquids as well as for gases. For incompressible liquids is $\partial \varrho / \partial t = 0$ and ϱ is furthermore spatially constant. The equation of continuity simplifies then to

$$\mathrm{div}(\boldsymbol{u}) = 0 \quad \begin{matrix} \textbf{(continuity equation for} \\ \textbf{incompressible liquids)} \end{matrix} \, . \tag{8.13a}$$

For the three components this equation reads

$$\frac{\partial u_x}{\partial x} + \frac{\partial u_y}{\partial y} + \frac{\partial u_z}{\partial z} = 0 \, . \tag{8.13b}$$

In pipes with constant cross section A the liquid flows only into one direction which we choose as the x-direction. Then $u_y = u_z = 0$ and (8.13b) becomes $\partial u_x / \partial x = 0 \Rightarrow u_x = \mathrm{const}$.

8.4 Bernoulli Equation

If a liquid or a gas flows in x-direction through a pipe with variable cross section $A(x)$ the flow velocity is larger at locations with smaller cross section (continuity equation). The volume elements therefore have to be accelerated and have a higher kinetic energy than at places with larger cross section. This results in a decrease of the pressure p. This can be seen as follows:

In order to transport the volume element $\mathrm{d}V_1 = A_1 \cdot \Delta x_1$ in the wider part of the pipe through the cross section A_1 it has to be shifted by Δx_1 against the pressure p_1 (Fig. 8.8). This demands the work

$$\begin{aligned} \Delta W_1 &= F_1 \Delta x_1 = p_1 A_1 \cdot \Delta x_1 \\ &= p_1 \Delta V_1 \, . \end{aligned} \tag{8.14a}$$

In the narrow part of the pipe is $\Delta V_2 = A_2 \cdot \Delta x_2$ and the work necessary to shift ΔV_2 by Δx_2 against the pressure p_2 is

$$\begin{aligned} \Delta W_2 &= p_2 A_2 \Delta x_2 \\ &= p_2 \Delta V_2 \, . \end{aligned} \tag{8.14b}$$

The kinetic energy of the volume elements is

$$E_{\mathrm{kin}} = \tfrac{1}{2} \Delta M \cdot u^2 = \tfrac{1}{2} \varrho \cdot u^2 \cdot \Delta V \, .$$

For ideal liquids (frictional forces are negligible) the sum of potential and kinetic energy has to be constant (energy conservation). This gives the equation

$$p_1 \Delta V_1 + \tfrac{1}{2} \varrho u_1^2 \Delta V_1 = p_2 \Delta V_2 + \tfrac{1}{2} \varrho u_2^2 \Delta V_2 \, . \tag{8.15}$$

For incompressible liquid is $\varrho =$ constant and therefore $\Delta V_1 = \Delta V_2 = \Delta V$. This simplifies (8.15) to

$$p_1 + \tfrac{1}{2} \varrho u_1^2 = p_2 + \tfrac{1}{2} \varrho u_2^2 \, . \tag{8.16}$$

For a frictionless incompressible liquid flowing through a horizontal pipe with variable cross section (Fig. 8.9) we obtain for a stationary flow from (8.16) the **Bernoulli Equation**

$$p + \tfrac{1}{2} \varrho u^2 = p_0 = \mathrm{const} \, . \tag{8.17}$$

The constant p_0 is the total pressure which is reached at locations with $u = 0$. the quantity $p_s = (\varrho/2) u^2 = p_0 - p$ is the **dynamic stagnation pressure (ram pressure)**, while $p = p_0 - p_s$ is the **static pressure** of the flowing liquid.

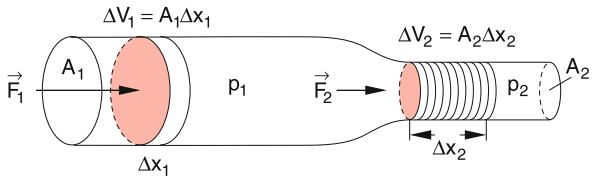

Figure 8.8 Illustration of Bernoulli-equation

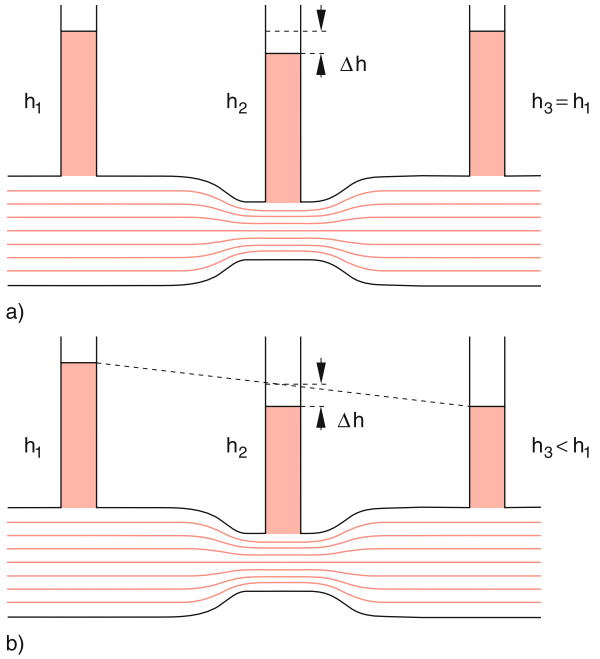

Figure 8.9 Demonstration of Bernoulli equation by pressure measurements in stand pipes. The pressure difference is $\Delta p = \varrho \cdot g \cdot \Delta h$. **a** For ideal liquids without friction; **b** for real liquids with friction. The liquid streams from *left to right*

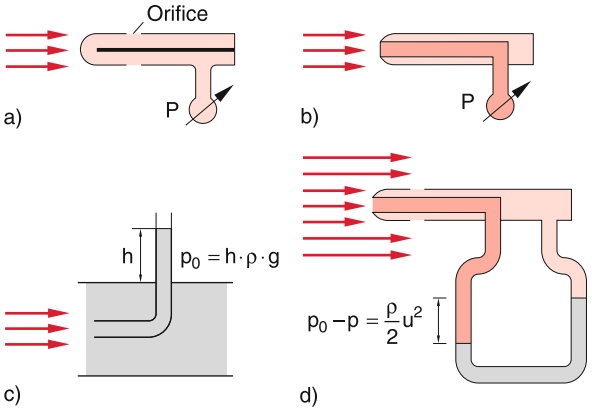

Figure 8.10 Measurement of pressure conditions in flows. **a** Measurement of static pressure; **b** measurement of total pressure p_0 with Pitot tube and pressure manometer; **c** measurement of p_0 with a stand pipe; **d** measurement of stagnation pressure $p_s = p_0 - p$ as difference of total pressure and static pressure

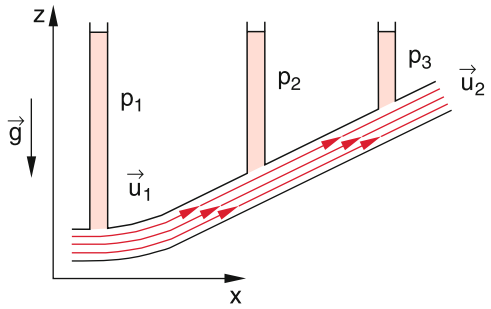

Figure 8.11 Flow of a liquid through an inclined pipe

The Bernoulli equation can be demonstrated with the arrangement shown in Fig. 8.9, where dyed water flows through a horizontal glass tube with variable cross section and vertical stand pipes. The rise h in the vertical stand tube gives the static pressure $p = \varrho \cdot g \cdot h$. At the narrow parts of the horizontal pipe the flow velocity is larger and therefore pressure and height h are smaller. In Fig. 8.9a the situation for an ideal frictionless liquid with $p(x) =$ constant for constant cross section is shown, while Fig. 8.9b illustrates the influence of friction on the pressure $p(x)$. For tubes with constant cross section a linear decrease of $p(x)$ is observed.

The three quantities p, p_0 and p_s can be measured at arbitrary locations in the flow with the devices shown in Fig. 8.10a–d. With a pressure gauge, shown in Fig. 8.10a which has a small hole in the sidewall of a tube, the liquid flow, streaming around the tube creates a static pressure inside the tube, which is monitored by a pressure manometer. The pitot-tube (Fig. 8.10b and c) has a hole at the end of the tube. If the tube is aligned parallel to the stream lines the flow velocity at the head of the tube is $u = 0$, i.e. the measured pressure is the total pressure p_0. It can be measured either with a manometer (Fig. 8.10b), or with a vertical stand pipe (Fig. 8.10c). With a combination of pressure gauge and Pitot tube (Fig. 8.10d) the pressure p_0 is measured at the head of the horizontal tube while a hole in the sidewalls monitors the pressure p. The difference $p_s = p_0 - p$ is shown as the difference of the heights of mercury in the U-shaped lower part of the device.

For liquid flows in inclined pipes the difference of potential energies $\Delta E_{pot} = \varrho \cdot g \cdot \Delta h \cdot \Delta V$ of a volume element ΔV at different heights h has to be taken into account. If the flow, for instance, is directed in the x-z-plane (Fig. 8.11) the height is $h = z(x)$ and we obtain from (8.17) the general equation

$$p + \varrho g z(x) + \tfrac{1}{2}\varrho u^2(x) = \text{const} = p_0 \,. \qquad (8.18)$$

For an ideal incompressible liquid ϱ is constant within the whole pipe. If the cross section of the pipe is constant also the flow velocity u is constant throughout the whole pipe. If $p + \varrho \cdot g \cdot z \geq p_0$ the flow ceases and $u = 0$ in the whole pipe.

Note: Although the Bernoulli equation (8.17) has been derived for incompressible liquids the equation allows to obtain also the pressure change of gases for laminar flows at not too high flow velocities. For example, inserting for air flows the numerical values $p_0 = 1$ bar, $u = 100\,\text{m/s}$, $\varrho = 1.293\,\text{kg/m}^3$ into the equation

$$p_0 - p = \tfrac{1}{2}\varrho \cdot u^2$$

one obtains $p = 0.935 p_0$, i. e. a pressure decrease of 6.5% and therefore also a corresponding decrease of the density ϱ. However, if the flow velocity approaches the velocity of sound ($c = 340\,\text{m/s}$) the change of the density becomes so large that the condition of incompressibility is even approximately not fulfilled.

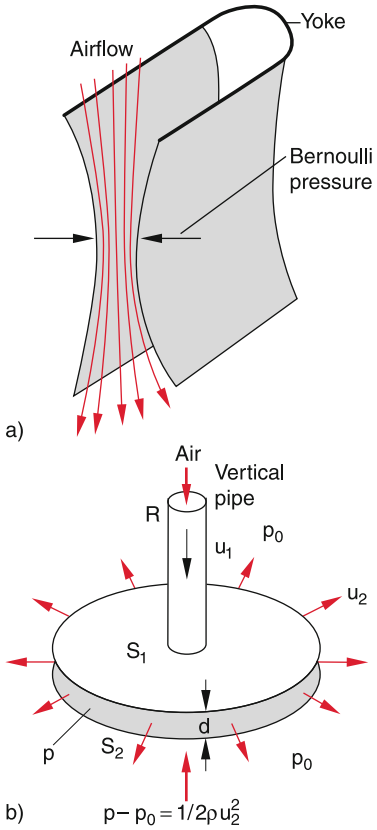

Figure 8.12 Hydrodynamic paradox: **a** Two curved aluminium plates, which can swing around a yoke, are pressed together when blowing air between them; **b** the lower circular plate is attracted to the upper plate when air is blown through the pipe

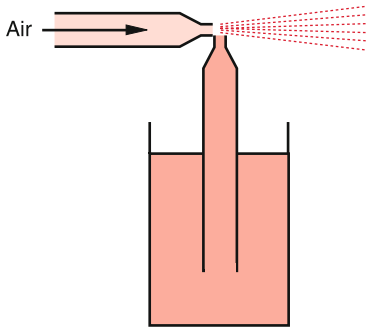

Figure 8.13 Vaporizer

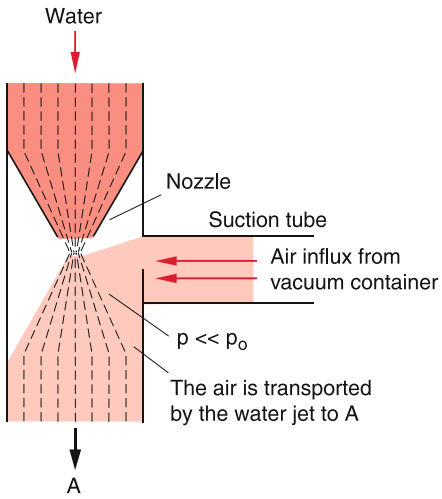

Figure 8.14 Water jet pump

The Bernoulli equation can be demonstrated by many simple experiments which often astound the auditorium. One example is the **hydrodynamic paradox**. Two curved aluminum plates are hanging on a U-shaped wire bar (Fig. 8.12a). If one blows air between the two plates they move towards each other, contrary to the expectation that they will be pushed away from each other. When air is blown through a vertical pipe fixed on one end to a circular disc S_1 with a hole (Fig. 8.12b) a second disc S_2 below the fixed disc is lifted to the upper disc by the air streaming between the two discs. The distance d between the two discs with area A must be below a critical value where the flow velocity u of the air is sufficiently large to cause an attractive force

$$F = A(p_0 - p) = \tfrac{1}{2}\varrho \cdot u^2 \cdot A \geq m \cdot g$$

between the two discs which can balance the weight $m \cdot g$ of the lower disc.

The Bernoulli theorem is used for many practical applications. Examples are the vaporizer or the spray bottle (Fig. 8.13) where air streams out of a narrow nozzle and generates a reduced pressure, which sucks the liquid out of the bottle into the air stream. Here it is nebulized. Another example is the water jet vacuum pump (Fig. 8.14). Here water streams with a large velocity through a narrow nozzle where it generates a reduced pressure. The air from the surrounding diffuses into the region with reduced pressure where it penetrates into the water jet and is transported out of the container into the outer space A, thus evacuating the container. With such a device reduced pressures down to 30 mbar can be achieved.

Undesirable effects of the Bernoulli theorem are the unroofing of houses under the action of typhoons (Fig. 8.15). When wind

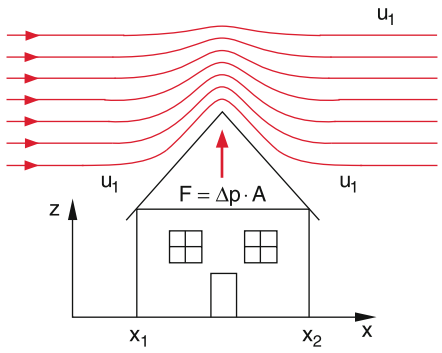

Figure 8.15 A strong wind can unroof a house due to the reduced pressure above the roof

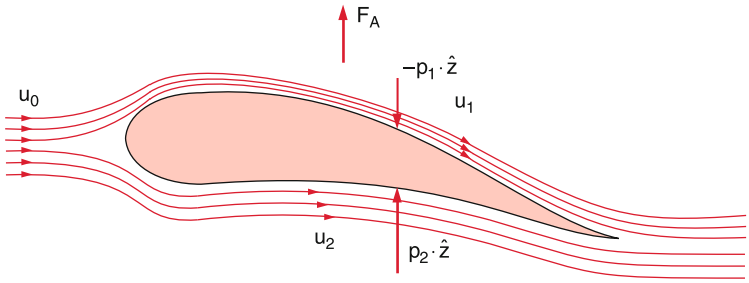

Figure 8.16 Aerodynamic lift at a wing profile due to the higher velocity around the upper side of the profile

blows with the flow velocity $u(x)$ over the roof of a house, the pressure difference $\Delta p = p_0 - p$ results in an upwards directed force

$$F = L_y \cdot \int \Delta p(x)\mathrm{d}x = L_y \cdot \int \tfrac{1}{2}\varrho u^2(x)\mathrm{d}x$$

on the roof, where L_y is the length of the roof in y-direction. The pressure difference depends on the flow velocity $u(x)$ which is maximum at the top of the roof, where the stream lines have the highest density.

The Bernoulli equation is the basis of the aerodynamic lift force and therefore important for the whole aviation. In Fig. 8.16 the profile of an airplane wing is shown with the stream lines of air flowing below and above the wing. For the asymmetric profile the air flows faster above than below the wing. This cause, according to (8.17) for a wing area A and the air density ϱ_a a lift force

$$F = (p_2 - p_1) \cdot A = \tfrac{1}{2}\varrho_L \left(u_2^2 - u_1^2\right) \cdot A \ .$$

Remark. Since air at high flow velocities is compressible and therefore cannot be treated as ideal liquid, the situation for a plane is more complex because the flow velocity of the air relative to the flying plane is very large. Besides friction forces turbulence and density changes play an important role for the calculation of the upwards lift (see Sect. 8.6).

8.5 Laminar Flow

Laminar flows (Fig. 8.3) are always realized when the frictional forces exceed the accelerating forces. Therefore, we will at first discuss the internal friction in liquids and gases and then illustrate the importance of laminar flow by several practical examples.

8.5.1 Internal Friction

Assume a plane sheet with area A in the y-z-plane is pulled through a liquid with the velocity u_0 into the horizontal direction (which we choose in Fig. 8.17 as the z-direction). The liquid layers at $x = x_0 \pm \mathrm{d}x$ adjacent to the two plate surfaces at $x = x_0$

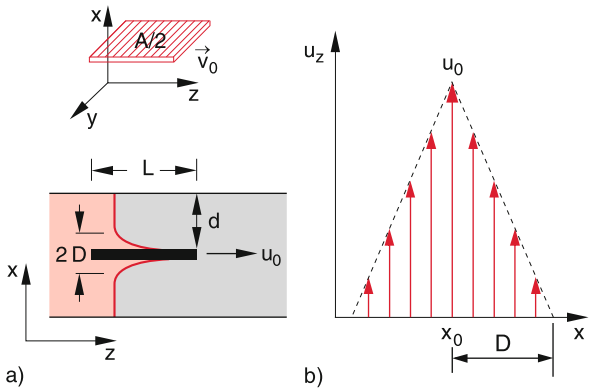

Figure 8.17 Internal friction of liquids. **a** A slab is pulled with the velocity u_x through a viscose liquid. It takes along boundary layers of the liquid. **b** Velocity profile and thickness D of the boundary layer

will be dragged with the moving plate due to the static friction between liquid and plate surfaces. These layers transfer part of their momentum $\varrho_L \cdot u_z \mathrm{d}V$ to the neighbouring liquid layers. This can be demonstrated by the experiment shown in Fig. 8.17a: In a glass trough is a viscous liquid, for example glycerine. The left part of the liquid is dyed. When an immersed plate is slowly pulled through the liquid with the velocity u_0 into the z-direction one can see that the liquid layers adjacent to the plate surfaces stick to the surfaces and are dragged with the velocity u_0. Perpendicular to the plate surfaces a velocity gradient is present (Fig. 8.17b). As has been discussed in Sect. 7.5, this gradient is due to the thermal motion of the liquid molecules, which penetrate by about a mean free path Λ into the neighbouring layers and transfer part of their momentum. This causes a velocity gradient $\mathrm{d}u/\mathrm{d}x$ perpendicular to the velocity of the plate.

In Sect. 7.5.4 it was shown, that the momentum transferred per second and unit area between neighbouring layers is $j_p = \eta \cdot \mathrm{d}u_z/\mathrm{d}x$. Since the time derivative of the momentum is equal to the acting force we obtain for the force between adjacent layers

$$F = \eta \cdot A \cdot \frac{\mathrm{d}u}{\mathrm{d}x} \ , \tag{8.19}$$

which appears when the plate is pulled with the constant velocity u_0 through the liquid, where A is the total surface of the plate (both sides!). This force must just compensate the friction force

Table 8.1 Dynamical viscosities of some liquids and gases at a temperature $T = 20\,^{\circ}\mathrm{C}$

Substance	$\eta/(\mathrm{mPa \cdot s})$
Water	1.002
Benzene	0.65
Ethanol	1.20
Glycerine	1480.0
Heavy fuel oil	660
Mercure	1.55
Air (10^5 Pa)	$1.8 \cdot 10^{-2}$
Helium (10^5 Pa)	$1.9 \cdot 10^{-2}$

opposite to the direction of u_0

$$F_\mathrm{f} = -\eta \cdot A \cdot \frac{\mathrm{d}u}{\mathrm{d}x} \,. \tag{8.20}$$

The factor η is the *dynamic viscosity*. It has the dimension $[\eta] = \mathrm{N \cdot s/m^2} = \mathrm{Pa \cdot s}$. In the older literature often the unit Poise $= \mathrm{P} = \mathrm{g \cdot cm^{-1} \cdot s^{-1}}$ is used. The conversion is $1\,\mathrm{P} = 0.1\,\mathrm{Pa \cdot s}$; 1 centipoise $= 1\,\mathrm{cP} = 10^{-3}\,\mathrm{Pa \cdot s}$.

In Tab. 8.1 the numerical values of η for some liquids are compiled. They should be compared with the data for gases in Tab. 7.3.

The dynamic viscosity η depends strongly on the temperature, as can be seen from Tab. 8.2. For liquid helium a superfluid phase exists at temperatures below 2.17 K, where $\eta = 0\,\mathrm{Pa \cdot s}$ [8.5].

The distance D where the liquid is dragged by the moving plate is called **fluid dynamic boundary layer**. Its value can be obtained by the following consideration: In order to move the plate by its length L against the frictional force F_f one has to accomplish the work

$$W_\mathrm{f} = -F_\mathrm{f} \cdot L = \eta A L \cdot \left|\frac{\mathrm{d}u}{\mathrm{d}x}\right| = \eta A L \cdot \frac{u_0}{D} \,, \tag{8.21}$$

where we have assumed that a linear velocity gradient $\mathrm{d}u/\mathrm{d}x = u_0/D$ is valid (Fig. 8.17b). The liquid layer with a mass $\mathrm{d}m$ and a velocity u has the kinetic energy $\mathrm{d}E_\mathrm{kin} = (1/2)\mathrm{d}m \cdot u^2$. With the constraint $u(x = \pm D) = 0$ the velocity of the layer is $u = u_0(1 - |x|/D)$. Altogether the kinetic energy of all dragged layers is

$$\begin{aligned} E_\mathrm{kin} &= \frac{1}{2}\int u^2 \mathrm{d}m = \frac{\varrho}{2}\int_0^D 2u_0^2\,(1 - |x|/D)^2\, A\,\mathrm{d}x \\ &= \frac{1}{3} A \varrho D u_0^2 \,. \end{aligned} \tag{8.22}$$

Due to friction part of the spent work is converted into heat. Therefore we get $E_\mathrm{kin} < W_\mathrm{f}$. This yields with (8.21) the relation

$$D < \left(\frac{3\eta L}{\varrho u_0}\right)^{1/2} \,. \tag{8.23}$$

The boundary layer has therefore the order of magnitude

$$D \approx \sqrt{\frac{\eta L}{\varrho u_0}} \,. \tag{8.24}$$

The boundary layer can only develop if the distance d to the container walls is larger than D. For $d < D$ the static friction between the liquid and the wall forces the velocity $u(d) = 0$, the dragged boundary layer becomes smaller and the velocity gradient larger.

For the derivation of the general friction force on a volume element $\mathrm{d}V = \mathrm{d}x \cdot \mathrm{d}y \cdot \mathrm{d}z$ we choose a liquid flowing into the z-direction with an arbitrary velocity gradient

$$\mathrm{grad}\, u_z = \left\{\frac{\partial u_z}{\partial x}, \frac{\partial u_z}{\partial y}, \frac{\partial u_z}{\partial z}\right\} \,.$$

We regard in Fig. 8.18 at first a flow that has only a gradient $\partial u_z/\partial x$ in x-direction ($\partial u_z/\partial y = \partial u_z/\partial z = 0$). The flow velocity $u_z(x)$ can be expanded into a Taylor series

$$u_z(x_0 + \mathrm{d}x) = u_z(x_0) + \frac{\partial u_z}{\partial x}\mathrm{d}x + \ldots \,, \tag{8.25}$$

which we truncate after the linear term.

The liquid layer between $x = x_0$ and $x = x_0 + \mathrm{d}x$ experiences a friction force $\mathrm{d}F_\mathrm{f}$ per surface element $\mathrm{d}A = \mathrm{d}y{\cdot}\mathrm{d}z$. If $\partial u_z/\mathrm{d}x > 0$ this force is decelerating for the surface layer at $x = x_0$ because here the neighbouring layer at $x = x_0 - \mathrm{d}x$ is slower but it is accelerating for the surface layer at $x = x_0 + \mathrm{d}x$, because here the adjacent layer is faster (Fig. 8.18b). The net tangential force is therefore

$$\begin{aligned} (\delta F_\mathrm{f})_z &= \mathrm{d}F_\mathrm{f}(x_0 + \mathrm{d}x) - \mathrm{d}F_\mathrm{f}(x_0) \\ &= \eta \cdot \mathrm{d}y\mathrm{d}z \left[\left(\frac{\partial u_z}{\partial x}\right)_{x=x_0+\mathrm{d}x} - \left(\frac{\partial u_z}{\partial x}\right)_{x=x_0}\right] \,. \end{aligned}$$

Inserting the derivatives from (8.25) yields for the bracket the expression $(\partial^2 u/\partial x^2)\cdot \mathrm{d}x$ and therefore for the net force onto the volume element $\mathrm{d}V$ due to the velocity gradient $\partial u_z/\partial x$

$$(\delta F_\mathrm{f})_z = \eta \cdot \mathrm{d}x\,\mathrm{d}y\,\mathrm{d}z \cdot \frac{\partial^2 u_z}{\partial x^2} = \eta \cdot \mathrm{d}V \cdot \frac{\partial^2 u_z}{\partial x^2} \,. \tag{8.26}$$

Table 8.2 Temperature dependence of the dynamical viscosity $\eta(T)$ of water and glycerine

$T/^{\circ}\mathrm{C}$	Viscosity $\eta(T)/(\mathrm{mPa \cdot s})$	
	Water	Glycerine
0	1.792	12 100
+20	1.002	1480
+40	0.653	238
+60	0.466	81
+80	0.355	31.8
+100	0.282	14.8

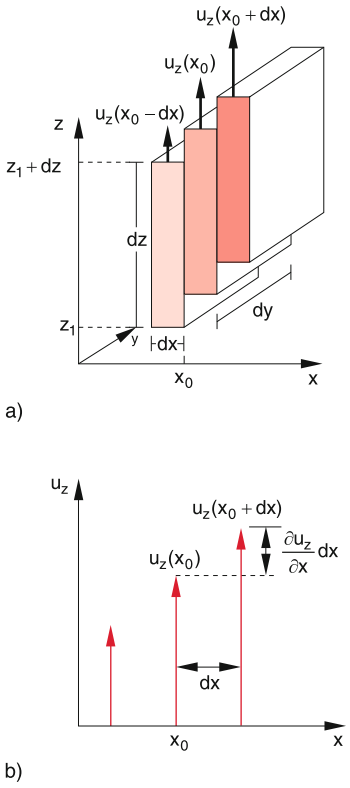

Figure 8.18 Derivation of friction force acting on a volume element dx dy dz in a flow with homogeneous velocity profile

A similar result is obtained for the velocity gradient $\partial u_z/\partial y$ in y-direction.

For compressible media, e.g. for gases, a velocity gradient $\partial u_z/\partial z$ can also appear for a flow into the z-direction if the density changes with z, while for incompressible media $\partial u_z/\partial z \neq 0$ only if the velocity changes, e.g. in tubes with variable cross section.

From (8.25)–(8.26) we finally obtain for the total friction force onto the volume element dV in case of a laminar flow with the velocity u_z the expression

$$(dF_f)_z = \eta\, dV \left(\frac{\partial^2 u_z}{\partial x^2} + \frac{\partial^2 u_z}{\partial y^2} + \frac{\partial^2 u_z}{\partial z^2} \right) . \qquad (8.26a)$$

The first two terms cause tangential forces (shear forces, see Sect. 6.2.3), the third term, which is only nonzero for compressible media causes a normal force onto the surface element $dx \cdot dy$. With the Laplace operator

$$\Delta = \frac{\partial^2}{\partial x^2} + \frac{\partial^2}{\partial y^2} + \frac{\partial^2}{\partial z^2}$$

(see Sect. 13.1.6) the total friction force onto the volume element dV, which moves with the velocity $\boldsymbol{u} = \{0, 0, u_z(x, y, z)\}$ can be written as

$$(dF_f)_z = \eta \cdot \Delta u_z dV . \qquad (8.26b)$$

For arbitrary flow velocities $\boldsymbol{u} = \{u_x, u_y, u_z\}$ (8.26b) can be generalized to

$$\boldsymbol{F}_f = \eta \cdot \int_V \Delta \boldsymbol{u}\, dV , \qquad (8.26c)$$

this is equivalent to the three equations $(F_f)_i = \eta \int \Delta u_i \cdot dV$ for the components $i = x, y, z$.

8.5.2 Laminar Flow Between Two Parallel Walls

In order to maintain a stationary flow with constant velocity into the z-direction between two walls at $x = -d$ and $x = +d$ one has to apply a force opposite to the friction force $\boldsymbol{F}_f$ which just compensates $\boldsymbol{F}_f$. This force can be, for instance, caused by a pressure difference between the planes $z = -z_0$ and $z = +z_0$. In the following we assume that the pressure is constant in a plane $z =$ constant, i.e. independent of x and y.

We consider in Fig. 8.19 a volume element $dV = dx \cdot dy \cdot dz$ with the width $dy = b$ in y-direction and the height dz. At its end faces $z = z_1$ and $z = z_1 + dz$ the pressure forces

$$dF_1 = b \cdot dx \cdot p(z_1) \quad \text{and} \quad dF_2 = b \cdot dx \cdot p(z_1 + dz)$$

are effective. They result in a total force onto the volume element dV

$$dF_z = -b\, dx \frac{dp}{dz} dz . \qquad (8.27)$$

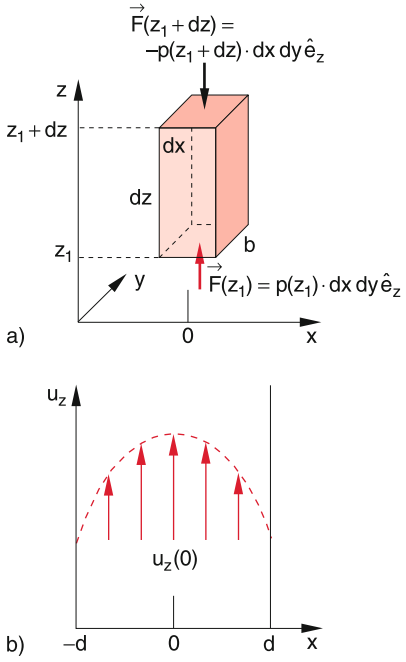

Figure 8.19 Laminar flow between two parallel walls

This pressure force compensates the friction force

$$(\mathrm{d}F_\mathrm{f})_z = \eta\,\mathrm{d}V\Delta u_z = \eta\,\mathrm{d}y\,\mathrm{d}x\,\mathrm{d}z\frac{\mathrm{d}^2u_z}{\mathrm{d}x^2}\ ,$$

if the condition

$$\frac{\mathrm{d}^2u_z}{\mathrm{d}x^2} = -\frac{1}{\eta}\frac{\mathrm{d}p}{\mathrm{d}z} \Rightarrow \frac{\mathrm{d}u_z}{\mathrm{d}x} = -\frac{x}{\eta}\cdot\frac{\mathrm{d}p}{\mathrm{d}z} + C_1$$

is fulfilled. The integration constant $C_1 = (\mathrm{d}u_z/\mathrm{d}x)_{x=0}$ gives the slope of the velocity profile $u(x)$ at $x = 0$.

Integration yields

$$u_z = -\frac{x^2}{2\eta}\frac{\mathrm{d}p}{\mathrm{d}z} + C_1x + C_2\ , \tag{8.28}$$

since p and $\mathrm{d}p/\mathrm{d}z$ do not depend on x.

For a liquid streaming between two parallel walls at $x = -d$ and $x = +d$ symmetry arguments demand $(\mathrm{d}u/\mathrm{d}x)_{x=0} = C_1 = 0$. At $x = \pm d$ the static friction between the liquid and the walls causes $u(x = \pm d) = 0$. This gives for the integration constant C_2

$$C_2 = \frac{d^2}{2\eta}\frac{\mathrm{d}p}{\mathrm{d}z}\ .$$

We then obtain for the velocity profile the parabola

$$u(x) = \frac{1}{2\eta}\frac{\mathrm{d}p}{\mathrm{d}z}(d^2 - x^2)\ , \tag{8.29a}$$

with the crest at $x = 0$ midway between the two walls. If the friction between the liquid and the walls is not high enough ($u(\pm d) \neq 0$), we get instead of (8.29a) the more general equation

$$u(x) = \frac{1}{2\eta}\frac{\mathrm{d}p}{\mathrm{d}z}(d^2 - x^2) + u_d\ . \tag{8.29b}$$

8.5.3 Laminar Flows in Tubes

The flow of liquids in cylindrical tubes plays an important role for many technical applications (water pipes, oil pipelines), and also in medicine (blood flow through veins). It is therefore worthwhile to study this problem in more detail.

We assume, as in the previous example, a pressure difference $p_1 - p_2$ between the planes $z = 0$ and $z = L$ in a cylindrical pipe with radius R (Fig. 8.20) which maintains a stationary flow. Symmetry reasons demand that the flow velocity can only depend on the distance r from the cylinder axis. For a coaxial small cylinder with radius r the same reasoning as in the previous section gives for the condition "friction force must compensate the pressure force"

$$-\eta\cdot 2r\pi\cdot L\frac{\mathrm{d}u}{\mathrm{d}r} = r^2\pi\cdot(p_1 - p_2)\ .$$

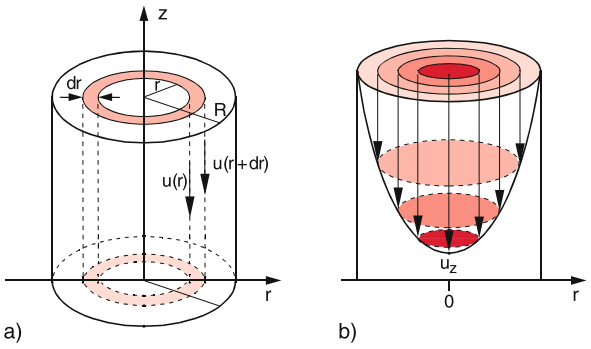

Figure 8.20 **a** Derivation of Hagen–Poiseuille law; **b** velocity profile of a laminar flow in a cylindrical tube

Integration over r yields

$$u(r) = \int_r^R \frac{p_1 - p_2}{2\eta L}r\,\mathrm{d}r = \frac{p_1 - p_2}{4\eta L}\cdot\left(R^2 - r^2\right)\ . \tag{8.30}$$

This velocity profile is a rotational paraboloid. It can be vividly demonstrated by the flow of coloured glycerine through a vertical pipe (Fig. 8.20b).

The total liquid volume flowing per second through the plane $z =$ constant of the hollow cylinder with radii between r_1 and $r_1 + \mathrm{d}r$ shown in Fig. 8.20a is according to (8.30)

$$\frac{\mathrm{d}}{\mathrm{d}t}(V(r)) = 2\pi r\,\mathrm{d}r\cdot u = \frac{2\pi r\,\mathrm{d}r\cdot(R^2 - r^2)}{4\eta L}(p_1 - p_2)\ .$$

The total volume streaming during the time t through the pipe is

$$\begin{aligned} V &= t\cdot\int_{r=0}^{R} 2\pi r\cdot u\,\mathrm{d}r \\ &= \frac{\pi R^4(p_1 - p_2)}{8\eta L}t = \frac{\pi R^4\Delta p}{8\eta L}t\ . \end{aligned} \tag{8.31}$$

The ratio $\Delta p/L = \partial p/\partial z$ is the linear pressure gradient along the tube. The total volumetric flowrate (volume per second) through the pipe is then

Hagen–Poiseuille Law

$$\frac{\mathrm{d}V}{\mathrm{d}t} = \frac{\pi R^4}{8\eta L}\Delta p = \frac{\pi R^4}{8\eta}\frac{\partial p}{\partial z} \tag{8.32}$$

Note the strong dependence of $\mathrm{d}V/\mathrm{d}t$ from the radius R of the pipe ($\sim R^4$!).

The human body utilizes this dependence for the regulation of the blood flow by adjusting the cross section area of the veins.

8.5.4 Stokes Law, Falling Ball Viscometer

When a ball with radius R is dropped with the initial velocity $u = 0$ into a liquid one observes at first an acceleration of the ball due to the gravity force and after a short falling distance a constant velocity. For this uniform motion the friction force F_f which increases with increasing velocity just cancels the gravity force

$$F_g = m_{\text{eff}} \cdot g = (\varrho_k - \varrho_{Fl}) \tfrac{4}{3}\pi R^3 \cdot g \qquad (8.33)$$

diminished by the buoyancy (Fig. 8.21).

Experiments with different liquids and balls with different radii prove that the friction force is proportional to the viscosity η of the liquid, to the radius R of the ball and to its velocity u. For radii still small compared to the diameter of the container one finds

Stokes Law

$$\boldsymbol{F}_f = -6\pi \cdot \eta \cdot R \cdot \boldsymbol{u}_0 \,. \qquad (8.34a)$$

The stationary final velocity u_0 is obtained for $\boldsymbol{F}_f + \boldsymbol{F}_g = 0$

$$u_0 = \frac{2}{9} g \frac{R^2}{\eta} (\varrho_K - \varrho_{Fl}) \,. \qquad (8.35)$$

Measuring u_0 allows the determination of the viscosity η, if the densities of liquid and ball and the ball radius R are known (Falling ball viscometer Fig. 8.22). According to (8.35) the ratio u_0/R^2 should be independent of the ball radius. This is indeed observed for small radii R.

Stokes Law (8.34a) can be derived also theoretically. A more detailed calculation [8.1a, 8.1b, 8.7] shows that (8.34) is only an approximation. The exact expression for the friction force, derived by *Oseen*, is

$$F_f = -6\pi\eta R \cdot u_0 \left(1 + \frac{3\varrho_{Fl} \cdot R \cdot u_0}{8\eta}\right) \,. \qquad (8.34b)$$

The second term in the bracket is for small radii R small compared to 1 and can be neglected.

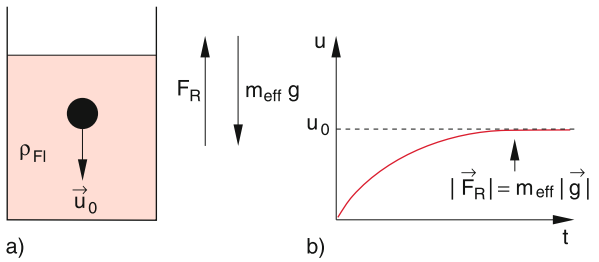

Figure 8.21 Uniform sink speed u_0 of a ball in a viscose liquid

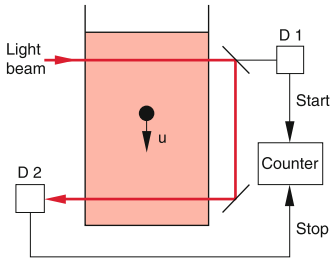

Figure 8.22 Viscosimeter with sinking ball and photoelectric barrier

Example

For steel balls ($\varrho = 7.8\,\text{kg/dm}^3$) with radius $R = 0.1\,\text{cm}$ falling in glycerine ($\varrho = 1260\,\text{kg/m}^3$) and $\eta = 1.48\,\text{Pa}\cdot\text{s}$, the stationary velocity becomes $u_0 = 1\,\text{cm/s}$. In this case the second term is $3.2 \cdot 10^{-3} \ll 1$. For $R = 1\,\text{cm}$, however, $u_0 = 1\,\text{m/s}$ and the second term becomes $2.5 > 1$ and cannot be neglected.

The Stokes Law (8.34a) therefore is correct only for sufficiently small products $R \cdot u_0$ of ball radius and final velocity u_0. ◀

8.6 Navier–Stokes Equation

In the previous sections we have discussed the different forces acting onto a volume element $\mathrm{d}V$ in a streaming liquid. We can now present the general equation of motion for a real viscous streaming liquid. With the different contributions

$$\begin{aligned} \mathrm{d}\boldsymbol{F}_f &= \eta \cdot \Delta\boldsymbol{u} \cdot \mathrm{d}V && \text{(friction force)} \\ \mathrm{d}\boldsymbol{F}_p &= -\mathbf{grad}\, p \cdot \mathrm{d}V && \text{(pressure force)} \\ \mathrm{d}\boldsymbol{F}_g &= = \varrho \cdot \boldsymbol{g} \cdot \mathrm{d}V && \text{(gravity force)} \end{aligned}$$

to the total force and the substantial acceleration (8.3)

$$\frac{\mathrm{d}u}{\mathrm{d}t} = \frac{\partial u}{\partial t} + (u \cdot \nabla)$$

we obtain the Navier–Stokes equation

$$\varrho \left(\frac{\partial}{\partial t} + \boldsymbol{u} \cdot \nabla\right) \boldsymbol{u} = -\,\mathrm{grad}\, p + \varrho \cdot \boldsymbol{g} + \eta \Delta \boldsymbol{u} \,. \qquad (8.36a)$$

For ideal liquids with $\eta = 0$ this reduces to the special case of the Euler equation (8.4). The friction term $\eta \cdot \Delta u$ expands the Euler equation, which is a first order differential equation, to a second order differential equation, which is more difficult to solve.

On the right hand side of (8.36a) the forces are listed and on the left hand side the motion induced by these forces, which we will now discuss in more detail.

The first term $\partial u/\partial t$ gives the time derivative of the velocity at a fixed location. The second term describes the change of the velocity of dV while it moves from the position r to $r + dr$. Using the vector relation

$$(u \cdot \nabla)\, u = \tfrac{1}{2}\,\mathrm{grad}\, u^2 - (u \times \mathrm{rot}\ u)\ , \qquad (8.36b)$$

that is deduced in textbooks on Vector Analysis [8.8, 8.9] (see also Sect. 13.1.6) we see that this spatial change of u can be composed of two contributions: The first term gives the change of the amount of $\boldsymbol{u}$, the second term the change of the direction of $\boldsymbol{u}$. This second term gives rise to vortices in the liquid, which we will discuss next.

8.6.1 Vortices and Circulation

When a liquid streams around a circular obstacle one observes for small velocities the streamline picture of laminar flow, shown in Fig. 8.5. If the velocity is increased above a critical velocity u_c, which depends on the viscosity η of the liquid, vortices appear behind the obstacle (Fig. 8.23). Such vortices can be made visible by small cork pieces floating on the liquid and moving along the streamlines. One observes that in a region around the centre of the vortex the liquid rotates like a rigid body. The rotational velocity

$$\boldsymbol{u} = \boldsymbol{\omega} \times \boldsymbol{r}$$

increases linear with the distance r from the centre and all particles have the same angular velocity ω. This region $r < r_k$ is called the **vortex kernel** (Fig. 8.24). Inserting small cork pieces with a fixed direction arrow to the surface of the liquid it becomes apparent that they turn once around their own axis while circulating around the vortex. (Fig. 8.25) as expected for a rigid rotation.

Outside of the vortex kernel ($r > r_k$) the angular velocity ω decreases with increasing distance r. The particles do no longer rotate about their axis but keep their spatial orientation (Fig. 8.25). This region of the vortex is called the **circulation**. Here a deformation of the volume elements during the rotation takes place (Fig. 8.26).

We can describe the vortex by the vortex vector

$$\boldsymbol{\Omega} = \tfrac{1}{2}\mathbf{rot}\,\boldsymbol{u}\ . \qquad (8.37)$$

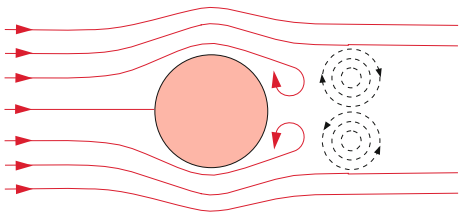

Figure 8.23 Generation of vortices in a turbulent flow around a circular obstacle

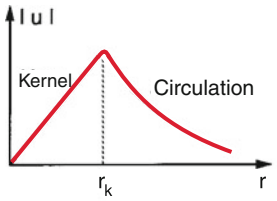

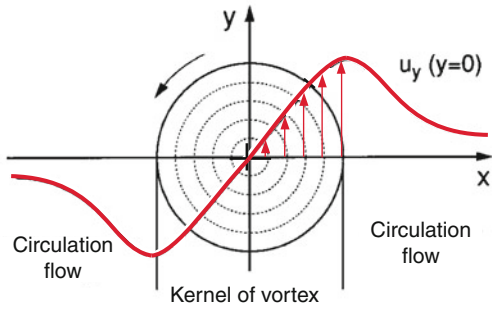

Figure 8.24 Kernel of vortex and circulation region

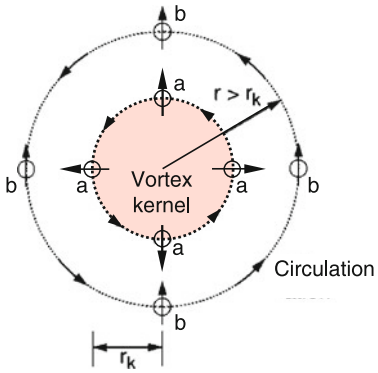

Figure 8.25 Orientation of cork pieces: **a** inside the vortex kernel (circular motion with turning orientation), **b** in the circulation region (non turning orientation)

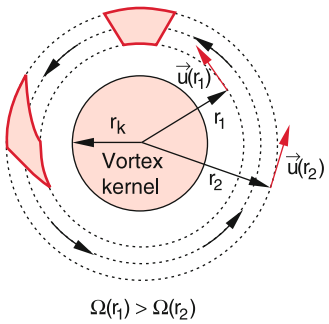

Figure 8.26 Deformation of a plane element in the circulation region outside the vortex kernel

The amount of $\boldsymbol{\Omega}$ gives the angular velocity ω inside the vortex kernel (see below). Magnitude and direction of $\boldsymbol{\Omega}$ in a vortex are generally not constant. They change because the vortex is not necessarily fixed in space but moves with the flowing liquid to

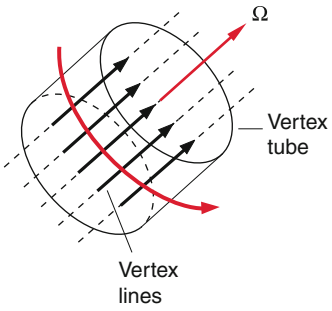

Figure 8.27 Vortex lines and tube

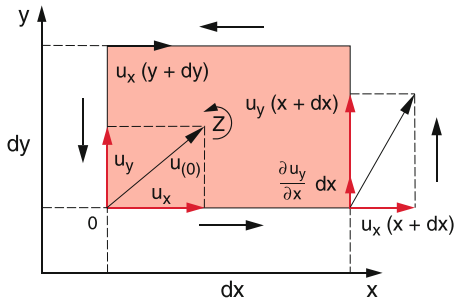

Figure 8.28 Explanation of circulation and its relation with rot *u*

other locations and furthermore the energy of the vortex changes because of friction and with it the magnitude of $\boldsymbol{\Omega}$ changes. The curves which coincide at every place with the direction of $\boldsymbol{\Omega}$ are called **vortex lines**. When, for instance, the particles move on circles in the x-y-plane the vector $\boldsymbol{\Omega}$ points into the z-direction. All lines parallel to the z-direction inside the kernel with $x^2 + y^2 \leq r_k^2$ are vortex lines (Fig. 8.27). All vortex lines through the vortex area A form the **vortex tube**.

For a quantitative description of torques based on the Navier–Stokes equation we have to study the rotational part $(\boldsymbol{u} \times \mathbf{rot}\,\boldsymbol{u})$ in (8.36a,b). At first we must understand, that the term rot $\boldsymbol{u}$ describes the rotation of moving particles. We therefore regard in Fig. 8.28 the tangential velocity components along the edge of the surface element $\mathrm{d}x \cdot \mathrm{d}y$. As a measure of the **torque strength** of the flow through the area A we define the circulation

$$Z = \oint \boldsymbol{u}\,\mathrm{d}\boldsymbol{s} \tag{8.38a}$$

along the edge of the surface in the counterclockwise direction. Our surface element $\mathrm{d}x \cdot \mathrm{d}y$ contributes the share

$$\begin{aligned} \mathrm{d}Z &= u_x\,\mathrm{d}x + \left(u_y + \frac{\partial u_y}{\partial x}\mathrm{d}x\right)\mathrm{d}y \\ &\quad - \left(u_x + \frac{\partial u_x}{\partial y}\mathrm{d}y\right)\mathrm{d}x - u_y\,\mathrm{d}y \\ &= \left(\frac{\partial u_y}{\partial x} - \frac{\partial u_x}{\partial y}\right)\mathrm{d}x\,\mathrm{d}y = (\mathrm{rot}\,\boldsymbol{u})_z \mathrm{d}x\,\mathrm{d}y \end{aligned} \tag{8.38b}$$

to the circulation, because the z-component of $\mathbf{rot}\,\boldsymbol{u} = \nabla \times \boldsymbol{u}$ is defined as $(\nabla \times \boldsymbol{u})_z = (\partial u_y/\partial x - \partial u_x/\partial y)$.

Analogous relations are obtained for the x- and y-components. From these relations one obtains by integration the Stokes' theorem

$$\oint \boldsymbol{u}\,\mathrm{d}\boldsymbol{s} = \int_A \mathrm{rot}\,\boldsymbol{u}\,\mathrm{d}\boldsymbol{A}\ , \tag{8.38c}$$

which states: "The surface integral over $\mathbf{rot}\,\boldsymbol{u}$ equals the path integral along the border of the surface element".

For a circular current of a liquid around a centre the circulation at a distance r from the centre is

$$Z = \oint \boldsymbol{u}\,\mathrm{d}\boldsymbol{s} = 2\pi r u(r)\ . \tag{8.38d}$$

The average amount Ω of the vortex vector $\boldsymbol{\Omega} = \frac{1}{2}\mathbf{rot}\,\boldsymbol{u}$ that points into the direction perpendicular to the surface is, according to Stokes' theorem

$$\begin{aligned} \boldsymbol{\Omega} &= \frac{1}{2A}\int |\mathrm{rot}\,\boldsymbol{u}|\,\mathrm{d}A = \frac{1}{2\pi r^2}\oint \boldsymbol{u}\mathrm{d}\boldsymbol{s} \\ &= \frac{2\pi r u}{2\pi r^2} = \frac{u}{r}\ , \end{aligned} \tag{8.38e}$$

where A is the area of the torque kernel.

Since the torque kernel rotates like a solid body, Ω must be independent of r. As illustrated in Fig. 8.24 the velocity $u = r \cdot \Omega$ increases linear with r.

The average $\Omega = Z/2A$ of the magnitude of the torque vector gives the circulation per surface unit and therefore the torque strength per surface unit.

8.6.2 Helmholtz Vorticity Theorems

For an ideal liquid ($\eta = 0$) the Navier–Stokes equation (8.36a) without external fields (gravity is neglected $\rightarrow g = 0$) can be transformed into an equation that illustrates certain conservation laws. This was first recognized in 1858 by Hermann von Helmholtz.

On both sides of (8.36a) we apply the differential operator **rot**, divide by the density ϱ and obtain from (8.36b) and (8.37) with $\mathbf{rot}\,\mathbf{grad}\,p = \nabla \times \nabla p = \mathbf{0}$ the equation (see Probl. 8.11)

$$\frac{\partial \boldsymbol{\Omega}}{\partial t} + \nabla \times (\boldsymbol{\Omega} \times \boldsymbol{u}) = \mathbf{0}\ . \tag{8.39}$$

Together with the equation of continuity $\mathrm{div}\,\boldsymbol{u} = 0$ (8.13) for incompressible media this equation determines completely and for all times the velocity field of an ideal streaming liquid. This means: If the quantities $\boldsymbol{\Omega}$ and $\boldsymbol{u}$ are given at a certain time (8.39) describes their future development unambiguously.

For example: If for $t = t_0$ the vortex vector $\boldsymbol{\Omega}$ for the total liquid is $\Omega = 0$, it follows from (8.39) $\partial\Omega/\partial t = 0$. This means: If an ideal liquid without vortices is set into motion it will stay vortex-free for all times.

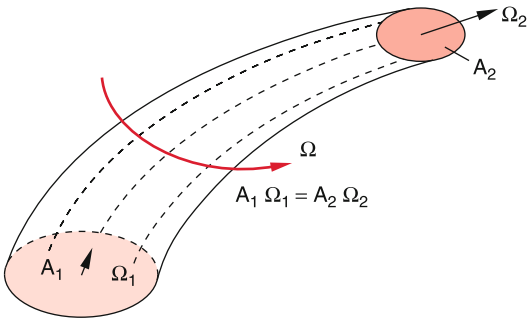

Figure 8.29 Deformation of a circular vortex during its flow with conservation of total mass and angular momentum

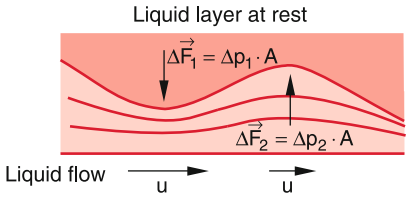

Figure 8.30 Generation of vortices by instabilities at boundaries between liquid layers with different velocities

If there are vortices in a liquid, it follows

$$\Omega = \tfrac{1}{2}\,\mathrm{rot}\,\boldsymbol{u} \Rightarrow \mathrm{div}\,\boldsymbol{\Omega} = \nabla \cdot (\nabla \times \boldsymbol{u}) \equiv 0\,. \qquad (8.40)$$

This means: Inside an ideal liquid, there are no sources or sinks for the vortex lines. They are either closed lines or they end at the boundary of the liquid, for instance at the walls of the liquid tube.

Inside an ideal liquid the vortex strength $Z = 2\boldsymbol{\Omega} \cdot \boldsymbol{A}$ is constant in time. Vortices cannot be generated nor vanish.

The constancy of Z in a frictionless liquid is equivalent to the conservation of angular momentum of the mass circulating in a vortex. Because of $\eta = 0$ no tangential forces can act and the pressure forces have only radial components. Therefore, there is no torque and the angular momentum has to be constant.

These conservation laws can be summarized by the following model: Vortices move like solid but strongly deformable bodies through a liquid or a gas. Without friction, their total mass and their angular momentum remain constant although the angular velocity and the radius of a vortex can change. This is illustrated in Fig. 8.29 by a cylindrical vortex. The constancy of the angular momentum $\boldsymbol{L} = I \cdot \boldsymbol{\omega}$ (see Sect. 5.5) with the moment of inertia $I = (1/2)Mr^2$ results in the equation

$$M_1 r_1^2 \Omega_1 = M_2 r_2^2 \Omega_2\,.$$

Since $M_1 = M_2$ and the vortex area $A = \pi \cdot r^2$ this gives

$$A_1 \cdot \Omega_1 = A_2 \cdot \Omega_2\,.$$

This means the vortex strength is constant.

8.6.3 The Formation of Vortices

In the previous section we have seen, that friction is essential for the formation of vortices. On the other hand, it was discussed in Sect. 8.5, that liquids with large friction show a laminar flow where no vortices occur. Vortices must be therefore formed in liquids with small viscosity where at certain places, e.g. at the boundaries with walls, the friction has maxima. Here velocity gradients occur between adjacent liquid layers because of the static friction between these liquid layers and the wall. These velocity gradients produce, due to friction, tangential forces, which give rise to vortices.

When such boundary layers show small irregularities as shown exaggerated in Fig. 8.30, the adjacent stream lines are deformed. At the narrow positions the stream lines are compressed and the flow velocity u increases. According to the Bernoulli equation, a pressure gradient Δp develops which further increases the irregularities. Finally, an unstable condition arises which results in the formation of vortices.

We will illustrate this vortex formation for the example of a flow around a circular cylinder (Fig. 8.31). For sufficiently small flow velocities u the influence of friction is small and a laminar flow occurs (Fig. 8.5 and 8.31a). At the stagnation point S_1 on the forefront of the cylinder, the flow velocity is zero and according to (8.17) the pressure equals the total pressure p_0. From S_1 the liquid moves along the upper side of the cylinder and is accelerated until it reaches the point P, where the velocity reaches its maximum and the pressure its minimum. The acceleration is caused by the pressure difference $\Delta p = p_0(S_1) - p(P)$. At the stagnation point S_2 at the backside of the cylinder the velocity becomes zero again, because the opposite pressure difference decelerates the flow and brings the velocity down to zero.

When the flow velocity is increased the velocity gradient between the wall and the adjacent liquid layers also increases. This increases the friction which is proportional to the velocity gradient. The liquid volume elements do not reach their full velocity in the point P and therefore reach the velocity $v = 0$ already in the point W before S_2 (Fig. 8.31b and 8.32). The pressure force caused by the pressure gradient between S_2 and W now accelerates the volume elements into the opposite direction against the flow velocity of the liquid layers farther away from the wall. There are two opposite forces acting on the liquid layers close to the wall (Fig. 8.32):

a the friction force due to the friction between the liquid layers close to the wall and the layers farther away which have different velocities,
b the force due to the pressure gradient.

These two forces exert a torque onto the liquid layers which cause a rotation. On each side of the cylinder a vortex is created. The two vortices have an opposite direction of rotation

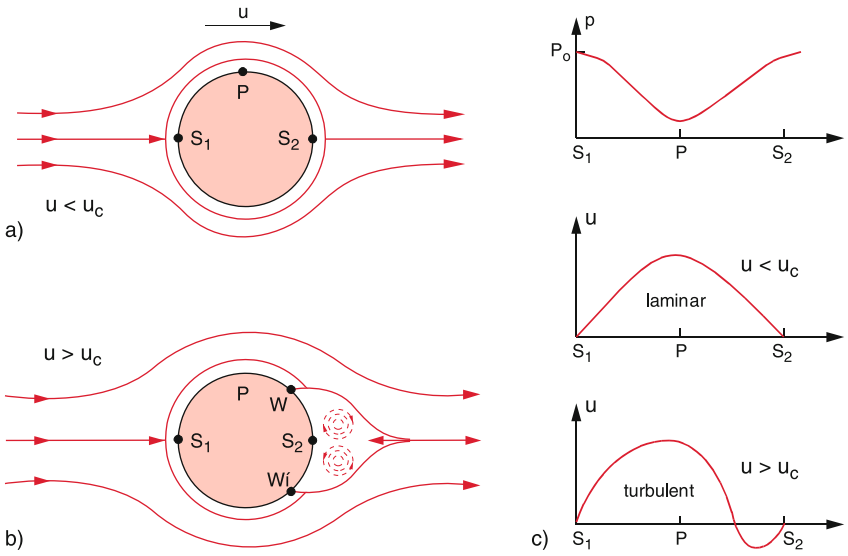

Figure 8.31 **a** Laminar flow for small velocities around a circular cylinder. **b** Generation of vortices behind a circular cylinder for large velocities. **c** Pressure and velocity behaviour for $u < u_c$ and $u > u_c$

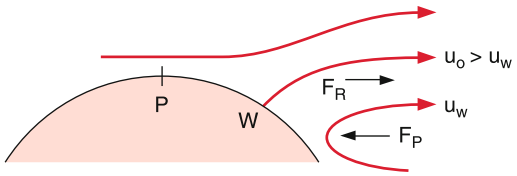

Figure 8.32 Illustration of torque necessary for the generation of vortices

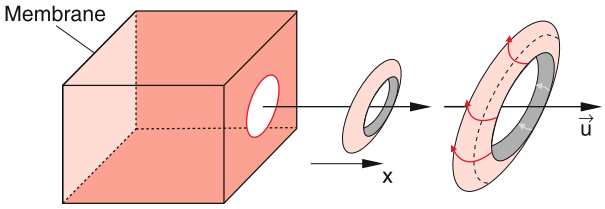

Figure 8.34 Generation of smoke vortex by beating a membrane at the backside of a box filled with smoke

(Fig. 8.31b), i.e. the vortex vector Ω_1 points into the direction into the drawing plane while Ω_2 points out of this plane.

These vortices can be visualized by dyed streamlines produced with the apparatus shown in Fig. 8.4.

Vortices can be also produced at the end of a circular tube, through which a liquid flows with sufficently high velocity (Fig. 8.33).

A nice demonstration experiment where vortices are produced in air mixed with cigarette smoke, is shown in Fig. 8.34. A box with a thin membrane at one side and a hole with 20–30 cm diameter on the opposite side is filled with cigarette smoke. Beating the membrane with a flat hand, produces a sudden pressure increase inside the box and drives the air-smoke mixture through the hole out of the box. At the edges of the hole vortices are produced which travel through the open air and can be readily seen by a large auditorium. These vortices can extinguish a candle flame, several meters away from the box. The vortices in air move nearly like a solid body through the air at atmospheric pressure. Without vortices a pure pressure wave would not be able to extinguish the candle flame because its intensity decreases with the distance d from the box as $1/d^2$ (see Sect. 11.9).

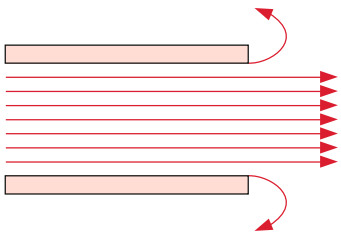

Figure 8.33 Generation of vortices at the end edge of a tube

8.6.4 Turbulent Flows; Flow Resistance

The curls shown in Fig. 8.31 behind an obstacle, do not stay at the location of their generation but move with the streaming liquid due to internal friction. At the original location new vortices can now emerge, which again detach from the surface of the immersed body and follow the liquid flow. This leads to the formation of a "Karman vortex street" (Fig. 8.35). It turns out that the two vortices of a vortex pair do not detach simultaneously but alternatively from the upper and the lower side of the obstacle. In the vortex street therefore the vortices with opposite angular momentum are shifted against each other. Car

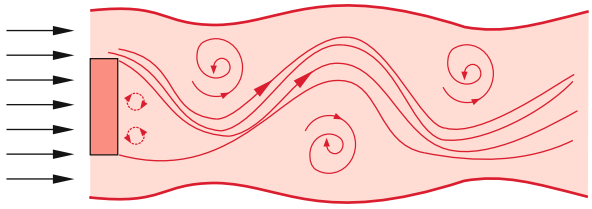

Figure 8.35 Karman vortex street

drivers can experience such a vortex street, when driving behind a fast truck, where they can feel the alternating directions of the transverse gust of winds. Behind a starting jet plane the vortex street can extend over several kilometres. Therefore there must be always a minimum safety distance between starting planes.

The rotational energy $E_{\text{rot}} = (I/2) \cdot \Omega^2$ (I = inertial moment), necessary for the generation of vortices has to come from the kinetic energy of the liquid flow. The flow velocity must therefore decrease when vortices are formed.

In a laminar friction-free flow the flow velocity $\boldsymbol{u}$ in the point S_2 in Fig. 8.31 is zero and in S_2 the same stagnation pressure p_0 appears as in S_1. In a turbulent flow the velocity behind the obstacle is not zero and therefore, according to the Bernoulli theorem the pressure is lower than p_0, causing a pressure difference between the regions before and behind the obstacle. This results in a force $F = \Delta p \cdot A$ on the obstacle with the cross section A in the direction of the flow. In order to keep the body at a fixed place, an opposite force has to be applied in addition to the force against the friction force.

The pressure difference at S_2 is according to Bernoulli's theorem $\Delta p \propto (1/2)\varrho \cdot u^2$. Therefore the force due to the pressure difference can be written as

$$F_{\text{D}} = c_{\text{D}} \cdot \frac{\varrho}{2} u^2 A \,, \tag{8.41a}$$

where the dimensionless constant c_{D} is the *pressure drag coefficient*. It depends on the form of the body (Fig. 8.36). This force adds to the friction force that is also present for laminar flows. According to the Hagen–Poiseuille law (8.31) the friction causes a pressure loss Δp_{f} (see Fig. 8.9b). The Bernoulli equation for a viscose liquid flowing through a horizontal tube, has to be augmented to

$$p_1 + \tfrac{1}{2}\varrho u_1^2 = p_2 + \Delta p_{\text{f}} + \tfrac{1}{2}\varrho u_2^2 \,; \quad \Delta p_{\text{f}} < 0 \,.$$

The pressure difference Δp_{f} depends on the square of the velocity u. We can write the total resistance force

$$F_{\text{total}} = F_{\text{f}} + F_{\text{D}} = \tfrac{1}{2} c_{\text{w}} \cdot \varrho \cdot u^2 \cdot A \,. \tag{8.41b}$$

The proportional factor c_{w} is called flow resistance coefficient. It depends analogue to c_{D} on the form of the body in the flow. In Fig. 8.36 the values of c_{w} for Air flows at atmospheric pressure are compiled for some profiles. This figure illustrates that the streamlined profile has the smallest flow resistance coefficient. Bodies with edges on the side of the incoming flow have larger flow resistance coefficients than spherical profiles.

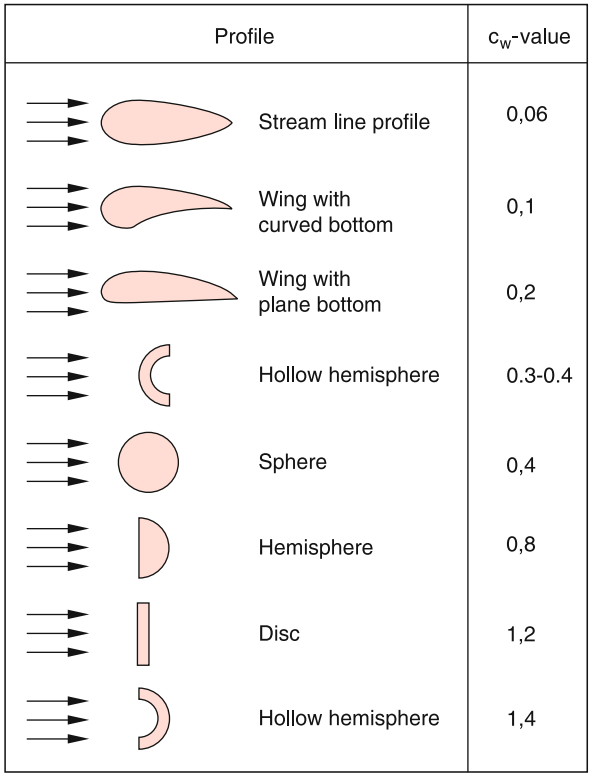

Figure 8.36 Flow resistance coefficents c_{w} for different shapes of obstacles

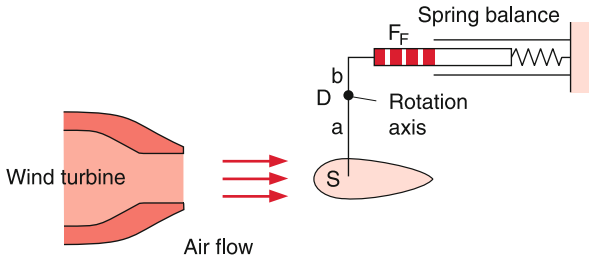

Figure 8.37 Experimental arrangement for the measurement of flow resistance

By means of the stagnation pressure $p_{\text{s}} = (1/2)\varrho \cdot u^2$ Eq. 8.41b can be written as

$$F_{\text{w}} = c_{\text{w}} \cdot p_{\text{s}} \cdot A \,. \tag{8.41c}$$

Experimental values of c_{w} can be measured with the arrangement shown in Fig. 8.37. The body to be measured is suspended by a bar that can turn around a horizontal axis. A fan blows air against the body. Due to its flow resistance the body is pressed to the right, thus expanding a spring balance on the other side of the bar. The torque exerted by the flow resistance of the body acting on the lever arm with length a is $F_{\text{w}} \cdot a$ where

$$F_{\text{w}} = \tfrac{1}{2} \cdot c_{\text{w}} \cdot \varrho \cdot u^2 \cdot A \,,$$

while the opposite torque of the spring balance is $F_{\text{s}} \cdot b$. The force F_{s} measured with the spring balance is a measure of the flow resistance F_{w} and allows the determination of the coefficient c_{w}.

8.7 Aerodynamics

The knowledge of all forces that are present when air streams around bodies with different shapes is very important not only for aviation but also for the utilization of wind energy and the optimization of car profiles. In this section only one aspect will be discussed, namely the aerodynamic buoyancy (lift) and its relation to the flow resistance of different body profiles. For a more extensive treatment, the reader is referred to the special literature [8.11a, 8.11b]

8.7.1 The Aerodynamical Buoyancy

In addition to the force on bodies in streaming media that acts in the direction of the flow also a force perpendicular to the streamlines can occur. We will illustrate this by two examples: In Fig. 8.38a we consider a laminar stream that flows around a circular cylinder. Because of symmetry reasons there could be no net force perpendicular to the current and only a force in the direction of the stream can occur which is caused by the friction between the flowing medium and the surface of the cylinder. However, if the cylinder rotates clockwise the relative velocity between surface and flowing medium is smaller at the upper side than at the lower side. This leads to a different friction on the two sides causing a net force upwards. This can be seen as follows: Due to friction a layer of the flowing medium close to the surface is dragged into the direction of the rotation causing a circulation of the layers close to the surface, which is partly transferred to adjacent layers (Fig. 8.38b).

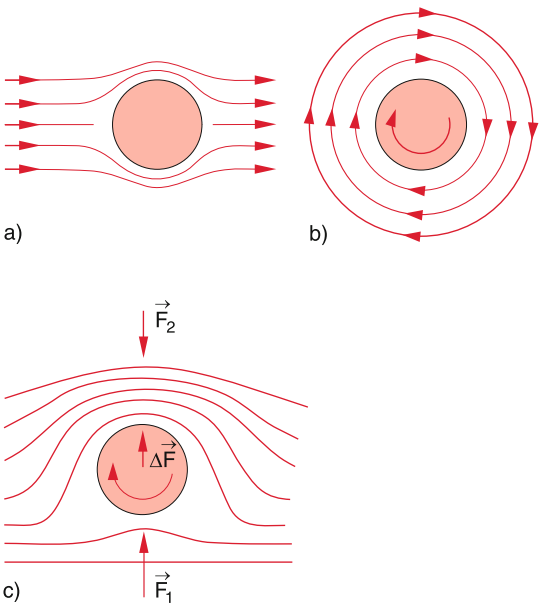

Figure 8.38 Magnus effect: **a** laminar flow around a circular cylinder, **b** circulation around a rotating cylinder in a liquid at rest, **c** streamlines around a rotation cylinder in an airflow as a superposition of **a** and **c**

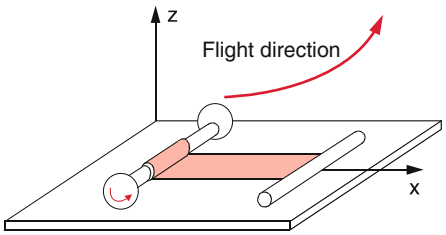

Figure 8.39 Demonstration of Magnus effect in air

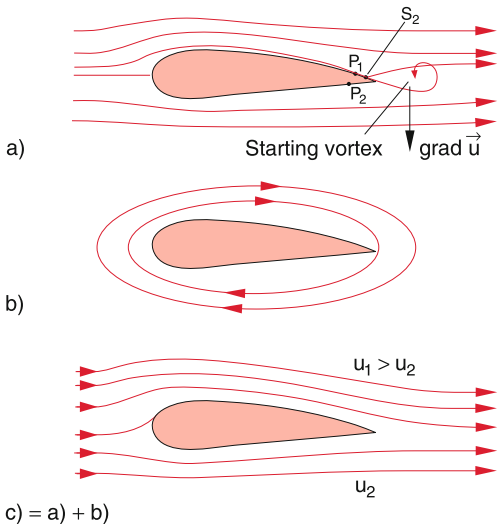

Figure 8.40 Generation of dynamical lift of a wing profile. **a** Without circulation; **b** With sole circulation; **c** Superposition of **a** and **b**

The superposition of this circulation and the laminar flow leads to an increase of the flow velocity on the upper side and a decrease on the lower side, resulting in the streamlines shown in Fig. 8.38c. The Bernoulli equation (8.17) tells us that this difference of the velocities results in a net upwards force $\Delta \boldsymbol{F} = \boldsymbol{F_1} - \boldsymbol{F_2}$ with $|\boldsymbol{F_1}| > |\boldsymbol{F_2}|$. This effect was first discovered by Magnus and was used for the propulsion of ships. The Magnus Effect can be demonstrated in Physics lectures with a hollow cylinder of cardboard that can be brought into fast rotation by a thin ribbon around the cylinder, which is fast pulled (Fig. 8.39). The cylinder moves then against the pulling direction and rises upwards because of the Magnus effect until its rotation is slowed down due to friction and then slowly sinks down.

For bodies with asymmetric profiles in a flowing medium a perpendicular net force occurs even without rotation of the body (dynamical buoyancy). It is again explained by the superposition of a circulation and the laminar flow. In this case, however, the circulation is not caused by rotation but by the formation of vortices. We will discuss this for the example of a wing profile (Fig. 8.40).

For a laminar flow around the asymmetric wing profile the layers of the flow medium close to the surface of the wing are decelerated due to friction. Because the path along the surface is

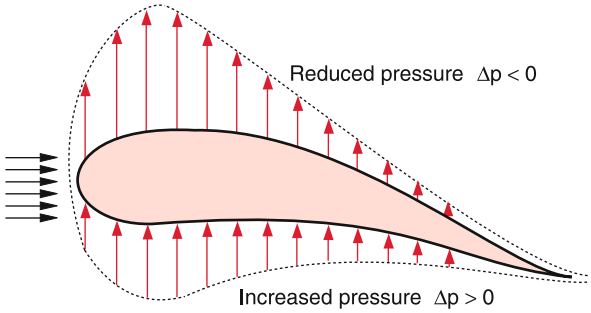

Figure 8.41 Distribution of lift force along lower and upper surface of a wing profile

longer at the upper side than at the lower side, the streaming medium arrives at the point P_1 at the upper side with lower velocity than at P_2 at the lower surface. The stagnation point S_2 at the backside is at the upper side behind P_1. Behind the profile a large velocity gradient grad u occurs between neighbouring layers of the streaming medium. If this gradient surpasses a limiting value, which depends on the velocity u and the viscosity η of the medium, a vortex develops behind the wing profile.

This can be demonstrated, when the profile is moved with increasing velocity through air or a liquid at rest. Above a critical velocity u_c the generation of a vortex is observed (starting vortex). Since the total angular momentum of the streaming medium must be conserved, the angular momentum of this vortex has to be compensated by a circulation around the total profile with opposite direction of rotation. (Fig. 8.40b). The superposition with the laminar flow leads, analogous to Fig. 8.38c, to an increase of the velocity above the wing profile and a decrease below the wing (Fig. 8.40c). According to the Bernoulli equation (8.17) this generates an upward force with the amount

$$F_L = \Delta p \cdot A = c_L \cdot \frac{\varrho}{2} \cdot \left(u_1^2 - u_2^2\right) A \,, \qquad (8.42)$$

which is called the **aerodynamical lift**.

The lift coefficient c_L depends on the shape of the profile. With pressure probes, the pressure distribution along the wing profile can be measured. Figure 8.41 shows a typical pressure distribution (difference Δp to the pressure in the surrounding air) along the upper and lower side of a wing profile, where the length of the arrows indicates the magnitude of Δp [8.12].

8.7.2 Relation between Dynamical and Flow Resistance

The Eq. 8.41 and 8.42 show that the flow resistance F_D and the F_L are both proportional to the kinetic energy per unit volume of the medium streaming around the profile, where the proportionality constants c_D and c_L both depend on the shape of the profile and the smoothness of its surface.

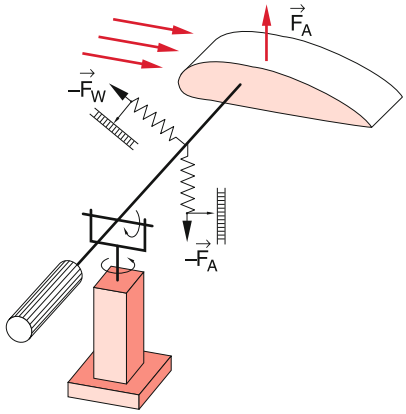

Figure 8.42 Arrangement for simultaneous measurements of flow resistance F_D and lift force F_L

Figure 8.42 shows a device (two-component balance) that allows the simultaneous measurement of the resistance force F_D and the lift force F_L for different model profiles.

It turns out that both forces (lift and drag) depend on the angle α of the profile relative to the laminar flow (Fig. 8.43). Even a flat plank shows for a certain range of α a lift force, which is, however, smaller than for a wing profile. The two curves $c_D(\alpha)$ and $c_L(\alpha)$ can be plotted in a polar diagram (Fig. 8.44) (polar profile) which illustrates the relation between c_D and c_L for all possible angles of attack. The optimum angel α is chosen such that the flow resistance is as small as possible, but the lift force is still high enough. If α is too large, vortices are generated at the upper side of the wing profile which decrease the flow velocity drastically and therefore reduce the force which can even become negative.

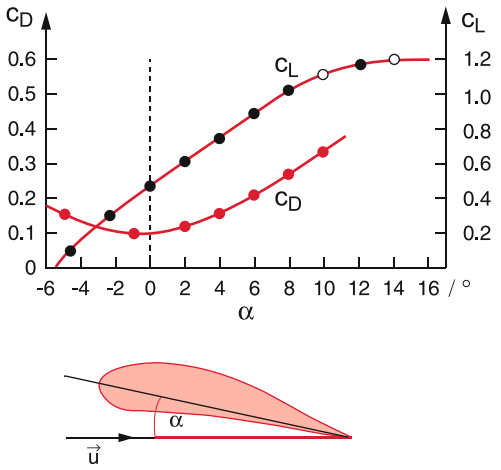

Figure 8.43 Dependence of flow resistance coefficient c_D and lift coefficient c_L on the angle of attack α of a wing profile

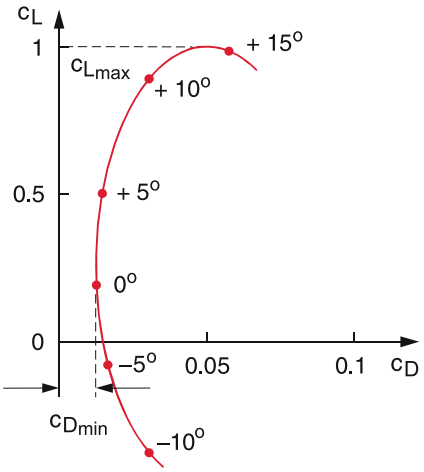

Figure 8.44 Polar diagram of a modern wing profile with small flow resistance coefficient

8.7.3 Forces on a flying Plane

At first we will discuss the flight without motor (glider). For a stationary flight of a glider with constant velocity $\boldsymbol{v}$ the total force on the glider (including gravity) must be zero. The total force is the vector sum of the lift force F_L, the flow resistance force F_D (Fig. 8.45) which depend on the flow velocity $u = -v$ of the air streaming around the glider, and the gravity force $m \cdot g$. A stable flight is only possible, if the glider flies on a declining path with the glide angle γ. From the condition $\boldsymbol{F} = \boldsymbol{0}$ we obtain with $F_D = |\boldsymbol{F}_D|$ and $F_L = |\boldsymbol{F}_L|$

$$\tan\gamma = -\frac{F_D}{F_L} \quad \text{and} \quad \sin\gamma = \frac{F_D}{mg} \,. \tag{8.43a}$$

The ratio F_D/F_L is called glide ratio. In order to realize a small glide angle, the force F_L should be as large as possible. As can be seen from Fig. 8.44 there is a lower limit for the glide ratio.

Modern gliders reach glide ratios of 1/50. This implies that a glider can reach 100 km flight distance without thermal lift, when it starts from a height of 2 km. If the glide angle γ is made larger by operating the elevation unit, the velocity v of the glider becomes larger, when γ is made smaller, the velocity decreases until the uplift breaks down and the glider becomes unstable. Without an experienced pilot, this might lead to a crash down.

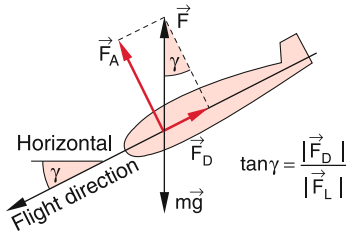

Figure 8.45 Forces at the gliding flight

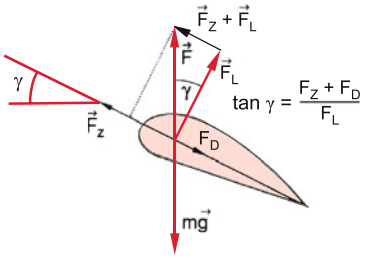

Figure 8.46 Forces at the ascent of a motor plane

When the air locally heats up (for instance above a hot ground or above chimneys of power stations) the air expands, its density decreases and it rises upwards (thermal lift, see Sect. 6.3). This gives an additional vertical component to the flow velocity of the air relative to the glider. In this case the glide angle γ can become negative, i.e. the glider rises upwards.

For planes with an engine (Fig. 8.46) an additional pulling force is produced by the propeller (or a corresponding propulsive force for jet planes). A climb is only possible, if the pulling force F_Z is larger than the magnitude of the opposite drag F_D. For the flight with constant velocity v at constant height the pulling force must just compensate the drag ($F_Z = F_D$). The angle of climb, γ is given by the ratio

$$\tan\gamma = \frac{F_Z - F_D}{F_L} \,. \tag{8.43b}$$

For $F_Z < F_D$ the angle γ becomes negative and the plane can fly with constant velocity only on a continuous descent.

8.8 Similarity Laws; Reynolds' Number

In Sect. 8.6.3 we have seen that vortices are caused by friction in the layers between liquid flow and walls. Although friction inside the liquid flow is small compared to that at the walls, it essentially influences the behaviour of the liquid flow, because this internal friction acts on the surface layers and starts turbulent flow.

Such boundary conditions are not included in the Navier–Stokes equation, because this equation describes the motion of an infinitesimal volume element and its motion under the influence of the different forces. It does not contain the special geometry of the flow pipe. Its geometry, however, plays an important role for the characteristics of the flow. It can be inserted into (8.36a) as special boundary conditions, but a reliable solution demands the knowledge of all details of such boundary conditions, which is often missing. Therefore generally experimental solutions are preferred which are obtained in the following way:

In hydro-and aero-dynamics the flow conditions for the motion of large objects (ships, airplanes) is studied with small models that have a similar but scaled down geometry. With such model

experiments in wind channels or in small liquid flow chambers, the optimum shape of a wing or a hulk can be found. In order to obtain realistic results, not only the shape of the model must be a true scaled down version of the true object, but also the flow conditions must be accordingly scaled down in a correct way. How this can be achieved, will be shortly outlined:

We normalize all length dimensions by a unit length L, all times by a unit time T and all velocities by L/T. We therefore define new values of length, time and velocity:

$$l' = l/L\,; \quad t' = t/T\,; \quad u' = u/(L/T) = u \cdot T/L. \tag{8.44a}$$

This gives for the gradient ∇' and the pressure p'

$$\nabla' = \nabla \cdot L\,; \quad p' = p \cdot (T/L)^2/\varrho\,, \tag{8.44b}$$

where $\nabla' = L \cdot (\partial/\partial x, \partial/\partial y, \partial/\partial z)$, L', t', u' and p' are dimensionless quantities.

With these normalized quantities the Navier–Stokes equation becomes

$$\frac{\partial \boldsymbol{u}'}{\partial t'} + (\boldsymbol{u}' \cdot \nabla')\,\boldsymbol{u}' = -\nabla' p' + \frac{1}{\mathrm{Re}}\Delta' \boldsymbol{u}'\,, \tag{8.45}$$

with the dimensionless Reynolds'-Number

$$\mathrm{Re} = \frac{\varrho \cdot L^2}{\eta \cdot T} = \frac{\varrho \cdot U \cdot L}{\eta}, \quad \text{with} \quad U = \frac{L}{T}\,. \tag{8.46}$$

The quantity $U = L/T$ is the flow velocity averaged over the length L. For ideal liquids is $\eta = 0 \rightarrow \mathrm{Re} = \infty$. Here the following statement can be made:

Flows of ideal liquids in geometrical similar containers for which (8.44) is valid, are described by the same equation (8.45) with the same boundary conditions. This means: At corresponding positions $\boldsymbol{r}'$ and times t' one obtains the same dimensionless quantities p' and u' in (8.45). Even non-stationary flows have the same progression within time intervals that are proportional to the container dimensions and inversely proportional to the flow velocity u.

For viscous liquids with $\eta \neq 0$ this is only valid if the Reynolds number Re has the same value. Flows of viscous liquids are only similar if the Reynolds number Re has the same value and the flow proceeds in containers with similar geometrical dimensions.

We will illustrate the physical meaning of the Reynolds number Re. When we multiply numerator and denuminator in the fraction (8.46) by $L^2 \cdot U$ we obtain

$$\mathrm{Re} = \frac{\varrho \cdot L^3 \cdot U^2}{\eta L^2 \cdot U} = \frac{2E_{\mathrm{kin}}}{W_{\mathrm{f}}}\,. \tag{8.47}$$

The numerator gives twice the kinetic energy of a volume element L^3, which moves with the velocity U, while the denominator is the friction energy W_{f}, which is dissipated when the volume element L^3 moves with the velocity U over a distance L.

For small Reynolds' numbers $E_{\mathrm{kin}} \ll W_{\mathrm{f}}$, which implies that the accelerating forces are small compared to the friction forces. The flow is laminar. Turbulent flows occur above a critical Reynolds' number $\mathrm{Re_c}$.

Experimental findings give for water flows in circular pipes with diameter d the critical Reynolds' Number

$$\mathrm{Re_c} = \varrho \cdot d \cdot U_{\mathrm{c}}/\eta = 2300\,.$$

For prevention of turbulent flows the normalized flow velocity must always obey the condition $U < U_{\mathrm{c}} \rightarrow \mathrm{Re} < \mathrm{Re_c}$. If Re is only slightly smaller than $\mathrm{Re_c}$ vortices are formed, which, however, have diameters that are smaller than the flow pipe diameter. Their rotational energy is small compared to the kinetic energy of the laminar flow and they therefore do not impede the flow very much. Only for $\mathrm{Re} \geq \mathrm{Re_c}$ their rotational energy becomes comparable to the friction energy and macroscopic vortices are generated. The flow becomes completely turbulent.

8.9 Usage of Wind Energy

The kinetic energy of streaming air can be utilized for the generation of electric power by wind energy converters. This had been already realized for many centuries by wind mills for grinding grain or for pumping water.

Modern wind converters generally have three rotor blades (coloured pictures 3 and 4). According to new insight in the flow conditions of air around the rotor blades, the shape of these rotors is formed in a complicated way in order to optimize the conversion efficiency of wind energy into mechanic rotation energy of the rotor, which is then further converted through transmission gears and electric generators into electric power.

Most of the wind energy converters produce alternating current, which is then rectified and again converted by dc-ac converters into alternating current. This is necessary in order to synchronize the phase of the ac-current with that of the countrywide network.

The kinetic energy of a volume element $\mathrm{d}V$ of the airflow moving with the velocity v is

$$E_{\mathrm{kin}} = \tfrac{1}{2}mv^2 = \tfrac{1}{2}\varrho v^2 \mathrm{d}V\,. \tag{8.48}$$

The air volume impinging per second onto the vertical area A is $\mathrm{d}V = v \cdot A$. The maximum power (energy per second) of the air flow hitting the area A is then

$$P_{\mathrm{W}} = \tfrac{1}{2}\varrho \cdot v^3 \cdot A\,. \tag{8.49}$$

In reality, only a fraction of the power can be converted into rotational energy of the wind converter. Firstly the wind is not completely decelerated to $v = 0$, because for $v = 0$ a tailback of air would build up behind the wind converter which would impede the air flow to the converter. Secondly, friction losses diminish the kinetic flow energy and rise the temperature.

If the velocity of the air inflow is v_1, it is decelerated to $v < v_1$ because of the stagnation at the rotor blades, where the pressure

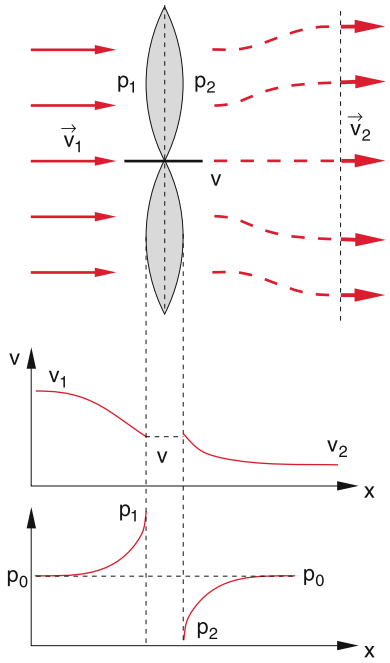

Figure 8.47 Schematic illustration of velocity and pressure conditions for a rotor blade at rest in an air flow [8.13]

increases from the initial value p_0 to $p_1 > p_0$ (Fig. 8.47). At the backside of the rotor the pressure sinks to $p_2 < p_0$. Behind the rotor the pressure increases again to p_0 and the airflow velocity is down to $v_2 < v$. Only after a larger distance behind the rotor the wind velocity rises again to its initial value $v = v_1$.

According to the Bernoulli equation is

$$p_1 - p_2 = \varrho \left(v_1^2 - v_2^2\right)/2 \,. \tag{8.50}$$

The force acting on the rotor blades with area A is

$$F = (p_1 - p_2)A = \varrho \left(v_1^2 - v_2^2\right) A/2 \,. \tag{8.51}$$

On the other hand this force can be written as

$$F = (v_1 - v_2)\mathrm{d}/\mathrm{d}t(mv) = (v_1 - v_2)\varrho v A \,. \tag{8.52}$$

The comparison between (8.51) and (8.52) shows that $v = (v_1 + v_2)/2$.

The power, transferred to the wind converter is then

$$\Delta P_\mathrm{w} = F \cdot v = \left(v_1^2 - v_2^2\right) \varrho v \frac{A}{2} = a \cdot P_\mathrm{W} \,. \tag{8.53}$$

Inserting P_w from (8.49) gives for the conversion factor a the value $a = (v_1 + v_2) \cdot (v_1^2 - v_2^2)/2v_1^3 < 1$. With a given initial velocity v_1 the maximum transferred power $\Delta P_\mathrm{w}(v_2)$ is reached for $\mathrm{d}(\Delta P_\mathrm{w})/\mathrm{d}v_2 = 0$. This gives with $v = (v_1 + v_2)/2$ the condition

$$-2v_2(v_1 + v_2)\varrho \cdot A/4 + (v_1^2 - v_2^2)\varrho \cdot A/4 = 0 \,,$$

which yields $v_2 = \frac{1}{3}v_1$.

For the efficiency factor a one obtains $a = 0.59$. This means that without any other losses at most 59% of the initial wind energy can be converted into rotational energy of the wind converter!

Example

$v_1 = 10\,\mathrm{m/s}$, $v_2 = 4\,\mathrm{m/s} \rightarrow v = 7\,\mathrm{m/s}$ and $a = 0.588$. A typical wind converter has rotor blades with $L = 50\,\mathrm{m}$ length and deliver several Megawatt electric power. At the rotational frequency $f = 1/\mathrm{s}$ the velocity of the rotor ends is already $300\,\mathrm{m/s} = 1080\,\mathrm{km/h}$, which is close to the limit of tensile strength of the blade material. ◀

Note, that the power transferred to the wind converter is proportional to the third power of the initial wind velocity. This means that already small changes of the wind velocity will cause large changes of the power available from wind converters. Modern wind converters can operate at wind velocities between 4 m/s and 25 m/s. For smaller velocities the transferred power is too small for a profitable operation. For higher velocities $v > 25\,\mathrm{m/s}$ the converters are shut down because of possible destruction.

The efficiency of the energy conversion is reduced by several losses. Firstly there are friction losses between different air layers with different velocities. They correspond to the friction losses η in the Navier–Stokes equation. Furthermore there are mechanical losses of the rotating blades and the transmission gear. Finally the losses in the electric generator have to be considered.

Figure 8.48 Offshore Windpark in the North Sea

Figure 8.49 Windfarm Krummhörn. Rotor span width is 30 m, the nominal electric power output is 300 kW per wind converter. (With kind permission of EWE corporation, Oldenbourg)

The available electric power is then

$$P_{\text{electric}} = a \cdot \eta_{\text{air}} \cdot \eta_{\text{mech}} \cdot \eta_{\text{electric}} \cdot P_{\text{w}} \ .$$

For our considerations about the wind velocities before and behind the wind converter we have assumed that the rotor blades are at rest. Because of their rotation the relative velocity between initial wind velocity and rotor velocity is smaller and the wind does no longer impinge perpendicular to the blades. This gives not only a smaller effective area $A_{\text{eff}} < A$ but also a smaller value of the transferred energy.

The power delivered by a wind converter, averaged over one year, is only between 10% and 40% of the installed power depending on the wind conditions at the converter location. The highest efficiency is reached for offshore wind converters (Fig. 8.48), because here the wind blows continuously and has generally a higher velocity than above undulating solid ground. For wind converters on solid ground the height should be as large as technically possible, because the wind velocity at 100 m altitude is much higher than directly above ground (Fig. 8.49).

In Tab. 8.3 the total installed electric power of wind converters is listed for the countries with the highest usage of wind energy and in Fig. 8.50 the impressive increase of worldwide annually new installed electric power from wind converters is illustrated.

Now we will discuss the energy conversion of wind converters in more detail: The forces driving the rotor blades can be composed of the flow resistance force and the Bernoulli-force. Their ratio depends on the shape of the blades and on their angle of attack α. This is similar to the situation for air flowing around a wing profile of an air plane (see Sect. 8.7.2 and Figs. 8.41 and 8.46). The pressure dependence $p(x)$ along a wing profile at rest is shown for the upper and lower side of the profile in Fig. 8.51. The pressure difference generates a lift force and a torque about an axis in x-direction. Depending on the orientation of the pro-

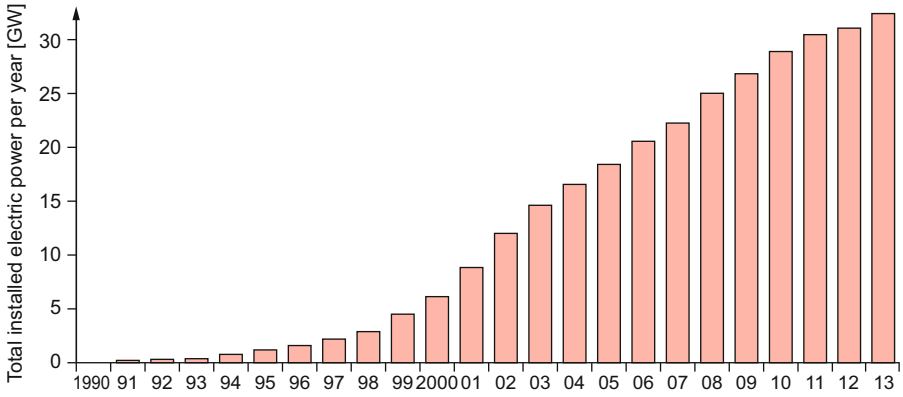

Figure 8.50 Growth of worldwide annually installed eletric power of wind converters in GW

Table 8.3 Installed electric power of wind converters for different countries (2014)

Ranking	Country	Power in GW
1	China	114.763
2	USA	65.879
3	Germany	39.165
4	Spain	22.987
5	India	22.465
6	UK	12.440
7	Canada	9.694
8	France	9.285
9	Italy	8.663
10	Brazil	5.939
11	Sweden	5.425
12	Portugal	4.914
13	Denmark	4.845
14	Poland	3.834
15	Australia	3.806
16	Turkey	3.763
17	Rumania	2.954
18	Netherland	2.805
19	Japan	2.789
20	Mexico	2.381
	Worldwide	369.553
	Europe	133.969

file against the direction of wind flow, the lift force as well as the flow resistance force can be used for driving the rotor blades.

When the rotor blade rotates with the angular velocity ω, the velocity $\boldsymbol{v}_B(r)$ of the section of the blade at a distance r from the rotation axis adds to the wind velocity v to an effective velocity $\boldsymbol{v}_{eff} = \boldsymbol{v} + \boldsymbol{v}_B(\boldsymbol{r})$ (Fig. 8.52). The angle of attack α against the direction of $\boldsymbol{v}_{eff}$ must be chosen in such a way (Fig. 8.43), that the optimum force can be used. Since $\boldsymbol{v}_{eff}$ changes with r the profile of the blade must change with r. With increasing r the blade must become slimmer and the direction of the profile changes. The whole blade is therefore twisted (Fig. 8.53) in order to reach for all sections of the rotating blade the optimum usage of the lift force.

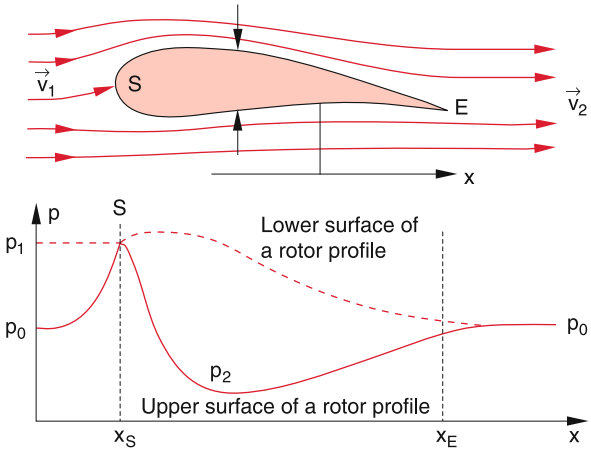

Figure 8.51 Pressure variation along the lower and upper surface of a rotor profile at rest, with air flowing around the profile. The rotation axis lies above the drawing plane [8.14]

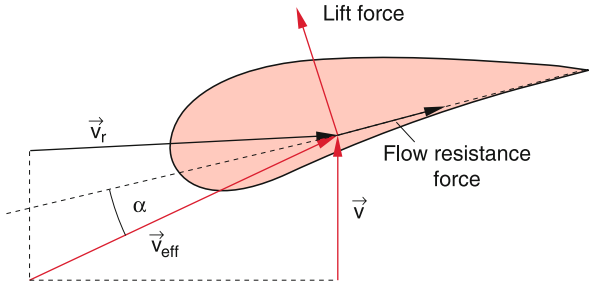

Figure 8.52 Velocities and forces on the rotating rotor. The rotation axis points into the direction of $\boldsymbol{v}$ and is above the drawing plane [8.13]

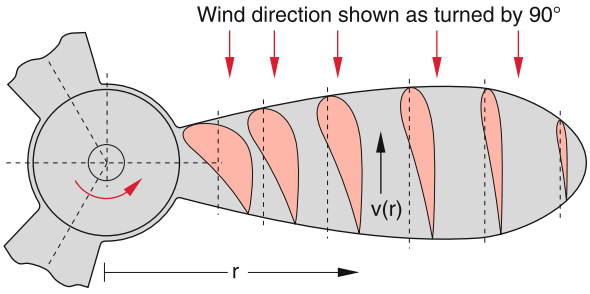

Figure 8.53 Rotor blade of a fast rotating wind converter. The *red areas* represent the rotor profile at different distances r from the rotation axis. In this drawing they are turned by 90° into the drawing plane. Also the wind direction is turned. The wind comes really from above the drawing plane

Summary

- The motion of particles of a flowing medium (liquids or gases) is determined by the total force $\boldsymbol{F} = \boldsymbol{F}_\mathrm{g} + \boldsymbol{F}_\mathrm{p} + \boldsymbol{F}_\mathrm{f}$ which is the vector sum of gravity force, pressure force and friction force. The equation of motion is

$$\boldsymbol{F} = \varrho \cdot \Delta V \cdot \frac{\mathrm{d}\boldsymbol{u}}{\mathrm{d}t} \,,$$

  where $\boldsymbol{u}$ is the flow velocity of the volume element ΔV with the mass density ϱ.
- In a stationary flow $\boldsymbol{u}(\boldsymbol{r})$ is at every position $\boldsymbol{r}$ constant in time but can vary for different positions $\boldsymbol{r}_i$.
- Frictionless liquids ($\boldsymbol{F}_\mathrm{f} = \boldsymbol{0}$) are called **ideal liquids**. For them the Euler equation

$$\frac{\partial \boldsymbol{u}}{\partial t} + (\boldsymbol{u} \cdot \nabla)\boldsymbol{u} = \boldsymbol{g} - \frac{1}{\varrho} \operatorname{grad} p$$

  describes the motion of the liquid.
- The continuity equation

$$\frac{\partial \varrho}{\partial t} + \operatorname{div}(\varrho \cdot \boldsymbol{u}) = 0$$

  describes the conservation of mass for a flowing medium. For incompressible media ($\varrho = \text{const}$) the continuity equation reduces to $\operatorname{div} \boldsymbol{u} = 0$.
- For frictionless incompressible flowing media the Bernoulli-equation

$$p + \tfrac{1}{2}\varrho \cdot u^2 = \text{const}$$

  represents the energy conservation $E_\mathrm{p} + E_\mathrm{kin} = E = \text{const}$. The pressure decreases with increasing flow velocity u.
  The Bernoulli equation is the basic equation for the explanation of the dynamical buoyancy and therefore also for aviation.
- For flow velocities u below a critical value u_c laminar flows are observed, while for $u > u_\mathrm{c}$ turbulent flows occur. This critical value u_c is determined by the Reynolds number $\mathrm{Re} = 2E_\mathrm{kin}/W_\mathrm{f}$ which gives the ratio of kinetic energy to the friction energy of a volume element $\Delta V = L^3$ when ΔV is shifted by L.
- For laminar flows where the inertial forces are small compared to the friction forces no turbulence occurs and the stream lines are not swirled.
- For a laminar flow through a tube with circular cross section πR^2 the volumetric flow rate

$$Q = \frac{\pi R^4}{8\eta} \operatorname{grad} p$$

  flowing per second through the tube is proportional to $R^4 \cdot \operatorname{grad} p$ but inversely proportional to the viscosity η.
- A ball with radius r moving with the velocity u through a medium with viscosity η experiences a friction force

$$\boldsymbol{F}_\mathrm{f} = -6\pi\eta r \cdot \boldsymbol{u} \,,$$

  that is proportional to its velocity $\boldsymbol{u}$.
- The complete description of a flowing medium is provided by the Navier–Stokes equation (8.36a) which reduces for ideal liquids ($\eta = 0$) to the Euler equation. The Navier–Stokes equation describes also turbulent flows, but for the general case no analytical solutions exist and the equation can be solved only numerically.
- For the generation and the decay of vortices friction is necessary. Vortices are generally generated at boundaries (walls and solid obstacles in the liquid flow).
- The flow resistance of a body in a streaming medium is described by the resisting force $F_\mathrm{D} = c_\mathrm{D} \cdot \varrho \cdot \frac{1}{2}u^2 \cdot A$. It depends on the cross section A of the body and its drag coefficient c_D which is determined by the geometrical shape of the body. The force is proportional to the kinetic energy per volume element ΔV of the streaming medium. In laminar flows, F_D is much smaller than in turbulent flows.
- The aero-dynamical buoyancy is caused by the difference of the flow velocities above and below the body. This difference is influenced by the geometrical shape of the body and can be explained by the superposition of a laminar flow and turbulent effects (circulation).

Problems

8.1 Estimate the force that a horizontal wind with a velocity of 100 km/h (density of air $= 1.225\,\mathrm{kg/m^3}$) exerts ($\varrho = 1.225\,\mathrm{kg/m^3}$; $c_D = 1.2$)
a) on a vertical square wall of $100\,\mathrm{m^2}$ area
b) on a saddle roof with $100\,\mathrm{m^2}$ area and length $L = 6\,\mathrm{m}$ and a cross section that forms an isosceles triangle with $\alpha = 150°$.

8.2 Why can an airplane fly "on the head" during flight shows, although it should experience according to Fig. 8.41 a negative buoyancy?

8.3 Why do the streamlines not intermix in a laminar flow although the molecules could penetrate a mean free path Λ into the adjacent layers?
Hint: Estimate the magnitude of Λ in a liquid.

8.4 Prove the relation (8.36b) using the component representation.

8.5 A cylinder is filled with a liquid up to the height H. The liquid can flow out through a pipe at height h (Fig. 8.54)

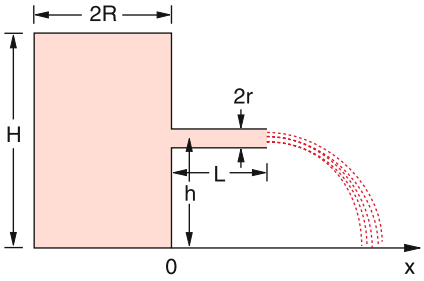

Figure 8.54 To Probl. 8.5

a) Calculate for an ideal liquid (no friction) the position $x(H)$ where the outflowing liquid hits the ground and the velocity $v_x(H)$ and $v_z(H)$ for $z = 0$. Compare this result with the velocity of a free falling body starting from $z = H$.
b) What is the function $z(t)$ of the liquid surface in the cylinder with radius R for a liquid with the viscosity η streaming through a pipe with length L and radius $r \ll R$ at the height $z = 0$?

8.6 A pressure gauge as shown in Fig. 8.10c is placed into flowing water. The water in the stand pipe rises by 15 cm. The measurement with the device of Fig. 8.10a shows a pressure of $p = 10\,\mathrm{mbar}$. How large is the flow velocity?

8.7 A funnel with the opening angle $\alpha = 60°$ is filled with water up to the height H. The water can flow into a storage vessel with volume V through a horizontal pipe at the bottom of the funnel with length L and inner diameter d.
a) What is the height $H(t)$ in the funnel as a function of time?
b) What is the total flow mass $M(t)$?
c) After which time is the funnel empty for $H = 30\,\mathrm{cm}$, $d = 0.5\,\mathrm{cm}$, $L = 20\,\mathrm{cm}$, and $\eta = 1.002\,\mathrm{mPa \cdot s}$?
d) After which time is the storage vessel with a volume $V =$ 4 litre full, if the water in the funnel is always kept at the height H by supplying continuously water?

8.8 A water reservoir has at Δh below the water surface a drain pipe with inner diameter $d = 0.5\,\mathrm{cm}$ and length $L = 1\,\mathrm{m}$ which is inclined by the angel α below the horizontal.
a) How much water flows per second through the pipe for a laminar flow with $\eta = 10^{-3}\,\mathrm{Pa \cdot s}$ and $\Delta h = 0.1\,\mathrm{m}$?
b) Above which angle α the flow becomes turbulent if the critical Reynolds number is 2300?

8.9 What is the minimum diameter of a horizontal tube with $L = 100\,\mathrm{m}$ to allow a laminar flow of water of $11 \cdot \mathrm{s^{-1}}$ from a vessel with a water level 20 m above the horizontal tube?

8.10 What is the vertical path $z(t)$ of a ball with radius r falling through glycerine ($\eta = 1480\,\mathrm{mPa \cdot s}$) if it immerses at $t = 0$ and $z = 0$ into the glycerine with the initial velocity $v_0 = 2\,\mathrm{m/s}$
a) for $r = 2\,\mathrm{mm}$,
b) for $r = 10\,\mathrm{mm}$?

8.11 Derive the Helmholtz equation (8.39) starting from (8.36a).

References

8.1a. G. Birkhoff, *Hydrodynamics.* (Princeton Univ. Press, 2015)

8.1b. E. Guyon, J.P. Hulin, *Physical Hydrodynamics.* (Oxford Univ. Press, 2012)

8.2. J.E.A. John, Th.G. Keith, *Gasdynamics.* (Prentice Hall, 2006)

8.3a. R.K. Bansal, *A Textbook on Fluid Mechanics.* (Firewall Media, 2005)

8.3b. G.K. Batchelor, *Introduction to Fluid Mechanics.* (Cambridge Univ. Press, 2000)

8.4a. J.P. Freidberg, *Ideal Magnetohydrodynamics.* (Plenum Press, 1987)

8.4b. P.A. Davidson, *An Introduction to Magnetohydrodynamics.* (Cambridge University Press, Cambridge, England, 2001)

8.5. F. Pobell, *Matter and Methods at Low Termperatures.* (Springer, Berlin, Heidelberg, 1992)

8.6. D. Even, N. Shurter, E. Gundersen, *Applied Physics.* (Pentice Hall, 2010)

8.7. A.E. Dunstan, *The Viscosity of Liquids.* (Hard Press Publ., 2013)

8.8. L. Brand, *Vector Analysis.* (Dover Publications, 2006)

8.9. K. Weltner, S. John, *Mathematics for Physicists and Engineers.* (Springer Berlin, Heidelberg, 2014)

8.10. G.B. Arfken, H.J. Weber, *Mathematical Methods for Physicists. A Comprehensive Guide.* (Elsevier Ltd., Oxford, 2012)

8.11a. L.J. Clancy, *Aerodynamics.* (Pitman, London, 1978)

8.11b. J.D. Anderson, *Fundamentals of Aerodynamics.* (McGrawHill, 2012)

8.12. D. Pigott, *Understanding Gliding.* (A&C Black, London)

8.13. M. Diesendorf, *GreenhouseSolutions with sustainable Energy.* (University of New South Wales, 2007)

8.14. J.F. Manwell, J.G. McGowan, A.L. Rogers, *Wind Energy Explained: Theory, Design and Applications.* (Wiley, 2010)

8.15. R. Ferry, E. Monoian, *A Field Guide to Renewable Energy Technologies.* (Society for Cultural Exchange, 2012)

8.16a. T. Burton et al., *Wind Energy Handbook.* (Wiley, 2001)

8.16b. N. Walker, *Generating Wind Power.* (Crabtree Publ., 2007)

8.17. The European Wind Energy Association, *Wind Energy: The Facts. A Guide to the Technology, Economics and Future of Wind Power.* (Routledge, 2009)